

<https://doi.org/10.3799/dqkx.2019.113>



粤西晚侏罗世花岗质岩体及其暗色微粒包体的成因及意义:年代学、矿物学和地球化学约束

刘梓¹, 张玉芝^{1,2,3*}, 崔翔^{1,2,3}, 甘成势^{1,2,3}, 王岳军^{1,2,3}

1. 中山大学地球科学与工程学院, 广东广州 510275

2. 广东省地球动力作用与地质灾害重点实验室, 广东广州 510275

3. 南方海洋科学与技术省实验室, 广东珠海 519082

摘要: 粤西阳江市八二花岗质岩体中广泛发育似斑状细粒闪长质暗色微粒包体, 这些暗色微粒包体形态多样, 与寄主岩具相似的矿物组合, 对研究花岗岩成因和壳—幔相互作用具有十分重要的意义。为了探讨它们的岩石成因及构造属性, 对寄主岩和暗色微粒包体开展了系统的岩相学、年代学和地球化学研究。LA-ICP-MS锆石U-Pb定年结果表明, 寄主岩年龄为160.0±1.0 Ma, 暗色微粒包体年龄为159.3±1.1 Ma, 均为晚侏罗世的产物。全岩地球化学特征显示, 寄主岩属于富钾的准铝质I型花岗岩, 寄主岩和暗色微粒包体均富集轻稀土元素和大离子亲石元素, 亏损重稀土元素和Nb、Ta、Ti等高场强元素。此外, 两者具相似的Sr-Nd同位素组成, 寄主岩的 $\epsilon_{\text{Nd}}(t)$ 值为-5.73~-5.67, ($^{87}\text{Sr}/^{86}\text{Sr}$)_i值为0.707 63~0.707 67; 而暗色微粒包体的 $\epsilon_{\text{Nd}}(t)$ 值为-5.81~-4.35, ($^{87}\text{Sr}/^{86}\text{Sr}$)_i值为0.707 04~0.707 74。锆石饱和温度计和角闪石全铝压力计表明八二花岗质岩体结晶于730~754 °C和19.8~20.6 km。综合寄主岩及其暗色微粒包体的岩石学、地球化学、同位素特征, 晚侏罗世八二花岗质岩体可能形成于陆内伸展背景, 由于软流圈物质上涌底侵, 导致中下地壳变基性岩为主的源岩部分熔融, 并且源区有少量幔源物质的加入, 局部可能存在岩浆混合作用; 暗色微粒包体是由镁铁质岩浆与长英质岩浆混合形成的。

关键词: 华南; 晚侏罗世; 暗色微粒包体; U-Pb年龄; 地球化学。

中图分类号: P59

文章编号: 1000-2383(2020)04-1243-23

收稿日期: 2019-05-19

Petrogenesis and Implications of the Late Jurassic Granitoid and Its Mafic Microgranular Enclaves in West Guangdong Province: Constraints from Geochronological, Mineralogical and Geochemical Evidence

Liu Zi¹, Zhang Yuzhi^{1,2,3*}, Cui Xiang^{1,2,3}, Gan Chengshi^{1,2,3}, Wang Yuejun^{1,2,3}

1. School of Earth Sciences and Engineering, Sun Yat-sen University, Guangzhou 510275, China

2. Guangdong Provincial Key Laboratory of Geodynamics and Geohazards, Guangzhou 510275, China

3. Southern Laboratory of Ocean Science and Engineering, Zhuhai 519082, China

Abstract: Mafic microgranular enclaves (MMEs) are widespread in the host granitoid from the Ba'er pluton in the west of the Guangdong Province. The MMEs have variable shapes and share similar mineral compositions with their host rocks, but are not fully understood. Petrographic study, zircon U-Pb dating and geochemical data are reported for the host granitoid and its MMEs,

基金项目: 国家自然科学基金项目(Nos.U1701641, 41830211); 中国科学技术部国家重点研发计划课题(No.2016YFC0600303); 广东省自然科学基金项目(No.2018B030312007)。

作者简介: 刘梓(1994—), 男, 硕士研究生, 构造地质学专业。ORCID:0000-0001-6366-3766. E-mail:liuz6@mail2.sysu.edu.cn

* 通讯作者: 张玉芝(1984—), 女, E-mail:zhangyuzhi@mail.sysu.edu.cn

引用格式: 刘梓, 张玉芝, 崔翔, 等, 2020. 粤西晚侏罗世花岗质岩体及其暗色微粒包体的成因及意义: 年代学、矿物学和地球化学约束. 地球科学, 45(4):1243—1265.

to constrain their petrogenesis and tectonic setting. LA-ICP-MS zircon U-Pb dating results yield weighted mean $^{238}\text{U}/^{206}\text{Pb}$ ages of 160.0 ± 1.0 Ma and 159.3 ± 1.1 Ma for the host rocks and the MMEs, respectively. The host granitoid is characterized by high SiO_2 (61.04% – 65.84%), K_2O (1.60% – 4.97%), low A/CNK(1.59 – 1.99), belonging to metaluminous, K-enriched I-type granitoid. Both host rocks and MMEs are enriched in LREE and LILE, and are depleted in HREE and HFSE (e.g., Nb, Ta and Ti). In addition, they also have indistinguishable Sr-Nd isotopic compositions. The granitoid has $\epsilon_{\text{Nd}}(t)$ values of -5.73 to -5.67 and $(^{87}\text{Sr}/^{86}\text{Sr})_t$ values of $0.707\ 63$ – $0.707\ 67$. The MMEs have $\epsilon_{\text{Nd}}(t)$ values of -5.81 to -4.35 and $(^{87}\text{Sr}/^{86}\text{Sr})_t$ values of $0.707\ 04$ – $0.707\ 74$. The calculated crystallization temperatures and depths of the Ba'er pluton are 730 – 754 °C and 16.8 – 20.6 km, respectively. According to comprehensive analysis of their tectonic settings as well as petrographic characteristics and geochemical data, the magma produced by partial melting of predominantly mafic middle-lower crust, with the input of minor mantle-derived materials, experienced different degrees of fractional crystallization in an intraplate extensional setting of Late Jurassic, Southeast China, which was accompanied by local magma mixing. The MMEs are generated by the mixing of the mafic magma with felsic magma.

Key words: South China; Late Jurassic; mafic microgranular enclave; U-Pb ages; geochemistry.

0 引言

花岗岩作为大陆地壳的重要组成部分,是研究大陆地壳形成、演化、增生和再造的重要对象,尽管花岗岩的组成矿物(石英、长石、云母等)相比其他岩石类型的更为简单,但是关于花岗岩形成演化的一系列问题仍然存在着不同观点(Chappell and White, 1974; 吴福元等, 2007; 陈璟元和杨进辉, 2015; Lee and Morton, 2015).而花岗岩中普遍存在暗色微粒包体(mafic microgranular enclaves, MMEs),这些MMEs常呈球状—椭球状,颜色一般较寄主岩更深,结构更为细粒,同时可以作为地球深部的岩石探针(莫宣学, 2011),蕴含着丰富的壳—幔物质及能量交换的信息.对寄主岩和MMEs系统的野外地质和地球化学方法研究,有助于笔者进一步了解它们的岩石成因、地球动力学背景、地壳深部的物质组成以及大陆地壳的生长和演化.国内外许多学者已对MMEs进行了大量工作(Jochum *et al.*, 1989; Didier and Barbarin, 1991; Elburg, 1996; Blake and Fink, 2000; 王德滋和谢磊, 2008; Shellnutt *et al.*, 2010; 彭卓伦等, 2011; Hu *et al.*, 2012; Zhao *et al.*, 2012; Pietranik and Koepke, 2014),但是关于它们的成因机制仍然存在较大争议,目前概括起来有以下4种:(1)岩浆在就位过程中围岩的捕掳体(Chen and Grapes, 2003);(2)源区岩石部分熔融过程中难熔物质的残留体(Chappell, 1996);(3)由同源岩浆早期矿物结晶分异而成(Clemens and Wall, 1988; Niu *et al.*, 2013; 牛之建等, 2014; Chen *et al.*, 2015);(4)幔源岩浆注入下地壳引起其熔融产生中酸性岩浆并与之发生

混合作用,MMEs是岩浆混合不彻底的产物(Barbarin, 2005; 朱金初等, 2006a; Perugini and Poli, 2012; Dan *et al.*, 2015; 秦拯纬等, 2018; 贾小辉等, 2018).

华南是世界上最大的花岗岩省之一,其中燕山早期花岗岩分布在长约1 000 km、宽约600 km的广大区域内,总出露面积超过64 000 km²(孙涛, 2006; Zhou *et al.*, 2006; Li *et al.*, 2007),岩性以黑云母花岗岩为主,含少量花岗闪长岩和白云母花岗岩.大多数燕山早期花岗岩的形成时间相对集中(~ 160 ~ 155 Ma),被称为中晚侏罗世“酸性大火成岩事件”(李献华等, 2007).长期以来,关于华南燕山早期花岗岩的研究受到了普遍的关注(Zhou and Li, 2000; Zhou *et al.*, 2006),特别是这些岩浆活动的形成机制和地球动力学背景一直是学术界高度关注和争论的重要问题.许多学者认为中生代古太平洋板块向欧亚大陆的俯冲造成了华南中生代的构造—岩浆活动,但是对太平洋俯冲的启动时间、俯冲角度及速率等方面存在着争议.Zhou and Li (2000)和Zhou *et al.* (2006)认为中侏罗世华南板块受古太平洋板块的低角度俯冲作用,随后俯冲板块逐渐后撤、俯冲角度逐渐变陡,这一过程可以解释华南地区晚中生代的岩浆活动.Li and Li (2007)认为古太平洋板块于晚二叠世开始向华南板块发生平板俯冲,并且在190~155 Ma发生板片拆沉作用,并以此解释华南大陆约1 300 km宽的褶皱构造带和岩浆活动.除此之外,关于华南晚中生代伸展或挤压的构造属性,目前存在着不同的认识,有的学者认为长期或多期次的伸展作用是华南晚中生代的主体构造体制(毛景文等, 2004),而有的学者认

为华南板块在晚中生代经历了2个旋回的收缩增厚和伸展减薄过程(崔建军等,2013)。李献华等(1997)通过对粤北白垩纪基性岩脉的年代学和地球化学研究认为,南岭乃至整个中国东南部燕山期区域构造经历了从侏罗纪的挤压到白垩纪拉张的转变。胡瑞忠等(2007)通过断陷盆地和变质核杂岩等方面的研究,也认为中国东南部晚中生代以来经历了多期次的拉张作用。张岳桥等(2012)对雪峰山地区的构造测量表明,该区经历了多期的挤压—伸展构造作用。对珠江口盆地的地球物理资料也表明了研究区多期的挤压—伸展构造(Ye *et al.*, 2018)。

郴州—临武断裂附近或以西的地区分布着许多燕山早期的花岗质岩体,包括花山—姑婆山(160~163 Ma;朱金初等,2006b)和骑田岭(153~165 Ma;朱金初等,2009)等岩体,并且这些岩体中发育丰富的MMEs。而在郴州—临武断裂以东鲜有燕山早期(~160 Ma)花岗质岩体及MMEs的报道。位于广东省阳江市雅韶镇的八二花岗质岩体中发育大量的MMEs,岩石露头新鲜,为相关研究提供了有利的条件。本文拟对八二花岗质岩体中的寄主岩和MMEs开展岩石学、矿物学、锆石U-Pb年代学、全岩主微量元素及Sr-Nd同位素研究,探讨它们的岩石成因及联系,为花岗岩的物质来源与成因机制提供新的制约,以期更好地理解该区域晚中生代构造背景及为壳幔演化提供岩石学证据。

1 地质背景和样品描述

华南板块位于东亚陆缘中段,濒临西太平洋,处在全球现今三大重要板块的汇聚拼合部位,并受到了西太平洋板块的西向俯冲,印—澳板块向北侧差异运动以及青藏高原隆升运动的影响(舒良树和周新民,2002;周新民,2003;张国伟等,2013)。研究区位于阳江市阳东县雅韶镇八二村,在阳江市城区南东方向约8 km处,出露地层主要包括寒武系、侏罗系、白垩系和第四系沉积物(图1b)。阳江市地理位置位于广东省西南沿海地区(图1a),大地构造上地处华南褶皱系西南段,云开隆起区东南缘,吴川—四会断裂的东侧,地势北高南低。该区地质构造较为复杂,新构造运动主要以周期性的垂直升降运动为主。境内出露地层从老到新有震旦系、寒武系、泥盆系、石炭系、二叠系、白垩系、第四系(广东省地质矿产局,1988)。区内岩浆岩分布较为广泛,发育多期岩浆侵入和喷发活动,其中以印支期和燕山期岩浆侵入活动为主,岩性包括黑云母花岗岩、花岗闪长岩和二长花岗岩等。

本文采样地点位于阳江市雅韶镇八二村村口公路旁,采样点坐标为21°47'33.5"N,112°03'48.0"E。八二花岗质岩体主要侵位于寒武系下亚群中,接触面一般为波状弯曲或港湾状,出露面积约8 km²,岩体中普遍发育MMEs,MMEs大部分分散产出,局

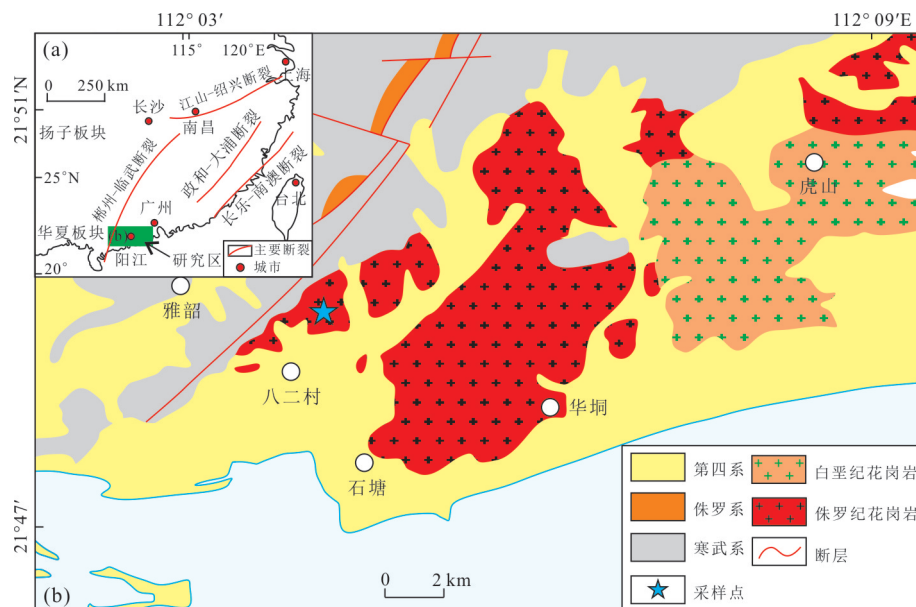


图1 研究区地质简图与采样点

Fig.1 Geological schematic map of the study area and sample location

图a据Wang *et al.*(2003);图b据广东省地质局(1964)1:20万地质图修改

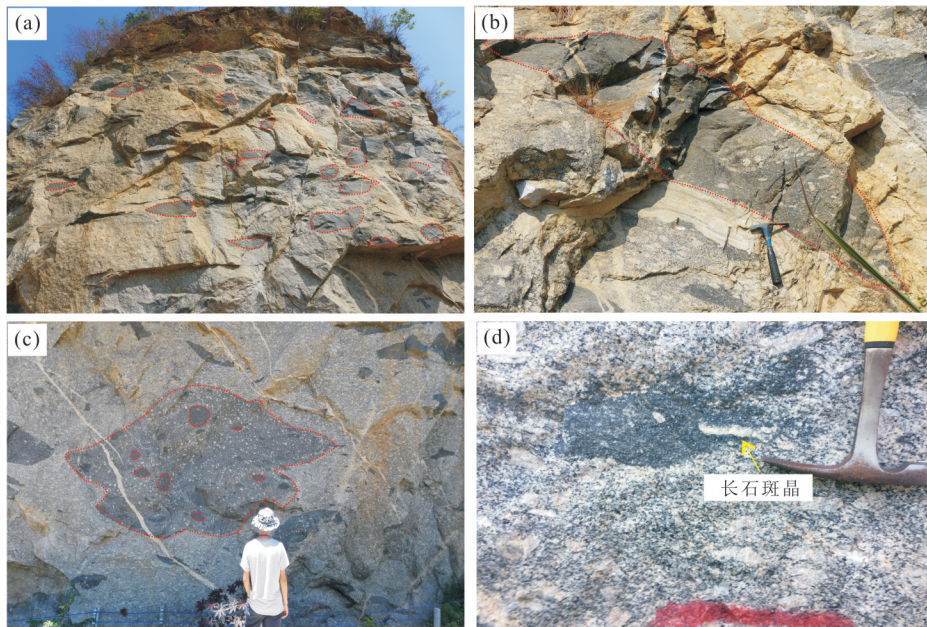


图 2 寄主岩与 MMEs 野外照片

Fig. 2 Field photographs of host rocks and mafic microgranular enclaves

a. 成群出现且大小不一的 MMEs; b. 纺锤状包体;c. 双包体;d. 寄主岩和 MMEs 交界处的长石斑晶

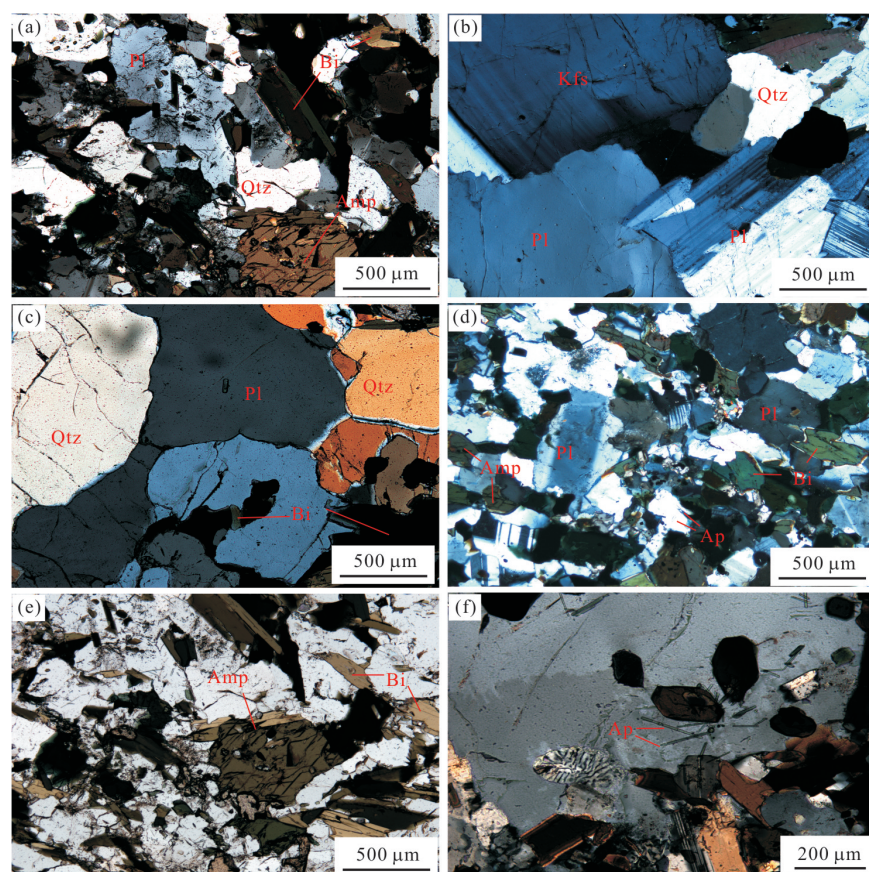


图 3 寄主岩与 MMEs 典型岩相学显微照片

Fig. 3 Photomicrographs of host rocks and mafic microgranular enclaves

a. 石英闪长岩显微照片;b. 二长花岗岩显微照片;c. 花岗闪长岩显微照片;d. MMEs 发育典型岩浆结构;e. 寄主岩中的角闪石等暗色矿物;f. MMEs 中的针状磷灰石。矿物名称缩写: Qtz. 石英; Pl. 斜长石; Bi. 黑云母; Amp. 角闪石; Ap. 磷灰石; Kfs. 钾长石

部比较密集,总体呈随机分布(图2a).MMEs大小各异,直径从几厘米到几十厘米不等,且形态多样,以浑圆状、纺锤状(图2b)、透镜状等为主,具塑性流变特征,同时可以观察到双包体现象(图2c),局部棱角状的包体少见.MMEs呈棱角状可能是其尚处于流变状态时接触到周围温度较低的花岗质岩浆,两者温差较大,MMEs迅速冷凝固结而形成.MMEs中存在大量的长石斑晶,可见处于MMEs和寄主岩界线上的长石(图2d),显示出长石迁移的过程.大多数MMEs与寄主岩的界线是截然的,本文采集的样品包括MMEs及其寄主岩.

寄主岩由石英闪长岩、二长花岗岩和花岗闪长岩组成.石英闪长岩呈半自形粒状结构,主要矿物有斜长石(55%~60%)、石英(10%~15%)、钾长石(10%)、黑云母(5%~10%)和角闪石(5%~10%)(图3a),副矿物有磷灰石、榍石等.二长花岗岩呈中一粗粒花岗结构(图3b),主要矿物有斜长石(25%~30%)、钾长石(25%~30%)、石英(20%~30%)、黑云母(5%~10%)和角闪石(3%~5%)(图3e),副矿物有磷灰石、榍石、磁铁矿和锆石等.花岗闪长岩呈中一粗粒花岗结构(图3c),主要矿物有斜长石(30%~35%)、石英(20%~30%)、钾长石(25%~35%)以及少量的黑云母和角闪石组成,副矿物有磷灰石、磁铁矿等,石英单偏光镜下为无色,呈不规则粒状,粒度多为1~5 mm,自形程度较差,有的可见波状消光,表面较干净;钾长石多为微斜长石及条纹长石,颗粒粗大,粒径多为3~7 mm;斜长石呈自形一半自形板状,粒径变化较大,约为2~7 mm,多具聚片双晶,偶尔发育环带结构;角闪石呈粒状,粒度约为2 mm左右,属普通角闪石,多色性明显;黑云母呈半自形片状,粒度约为0.3~0.5 mm,角闪石和黑云母分散分布于岩石中.

MMEs呈深灰色,似斑状结构,具典型的岩浆结构(图3d).MMEs与寄主岩中的矿物种类大致相同,主要由斜长石(50%~55%)、普通角闪石(10%~15%)、黑云母(15%~20%)、石英(3%~5%)及少量钾长石(3%~5%)组成,副矿物主要为磷灰石、榍石和不透明的铁氧化物等,磷灰石常出现在石英或者长石的内部,针状—短柱状均有出现(图3f).斜长石多呈板状,发育环带结构,可见较大的斜长石斑晶,粒度约为1.0~3.0 mm;角闪石呈半自形柱状、菱形状,粒度多为0.3 mm左右,单偏光镜下为浅绿色;MMEs的矿物粒度相比寄主岩来说要更细,同时相

比于寄主岩,MMEs相对贫石英和钾长石,富镁铁质矿物(角闪石和黑云母).

2 分析方法

2.1 LA-ICP-MS 锆石 U-Pb 定年

本文用于U-Pb定年的锆石全部选自新鲜的全岩样品,锆石的分选主要采用人工重砂法进行.首先,在双目显微镜下观察所分离锆石的特征,从中筛选出晶型好、无裂缝和透明度高的锆石作为测定对象.其次,将这些挑选的锆石颗粒使用无色透明的环氧树脂固定制成锆石靶并抛光至锆石的核部暴露出来.在进行测定前,在透射光和反射光条件下对锆石拍照;最后,使用扫描电子显微镜上的阴极发光仪进行阴极发光(CL)图像拍摄,用于观察锆石的内部结构并选择合适的锆石定年点位.锆石阴极发光成像(CL)分析在中山大学Carl ZEISS SIGMA场发射扫描电镜上完成.锆石U-Pb定年分析在中国科学院广州地球化学研究所同位素地球化学国家重点实验室完成,所用仪器包括美国Thermo Fisher Scientific公司的Neptune Plus型多接收电感耦合等离子体质谱仪(MC-LA-ICP-MS)和Resonetics公司的RESolution M-50型193 nm的激光剥蚀系统,关于仪器的详细介绍见Zhang *et al.*(2014).实验过程中激光束斑直径为24 μm,以He为载气.选用ICP-MS Data Cal 8.0软件对锆石分析信号进行选择、漂移校正和定量标准化(Liu *et al.*, 2009),锆石年龄谐和图采用Isoplot 3.0程序获得.

2.2 主、微量元素和Sr-Nd同位素分析

将新鲜岩石样品破碎成拇指大小的碎块之后,用5%的稀盐酸溶液在超声波条件下清洗,以淋滤掉碳酸盐矿物,然后用清水冲洗干净.将岩石碎块在玛瑙研钵中研磨成小于200目的粉末,这些粉末用于全岩主、微量元素和Sr-Nd同位素分析.全岩主、微量元素分析和Sr-Nd同位素测定实验均在中国科学院广州地球化学研究所同位素地球化学国家重点实验室完成.全岩主量元素分析采用碱熔玻璃片方法,通过型号为Rigaku 100e型波长色散型光谱仪(XRF)测定,具体的分析流程参见文献(李献华等,2005),分析误差1%~5%.微量元素分析采用PerkinElmer Elan6000型质谱仪进行测试,该仪器的分析精度一般优于5%,用HNO₃和HF对样品粉末进行初步溶解,然后将其放到钢套中高温高压溶解48 h,将难溶物质溶解掉,详细的分析流程参见文献刘颖和刘海

臣(1996).利用阳离子树脂交换柱对Sr和Nd元素进行提取,用盐酸作为淋洗液.Sr-Nd同位素比值测定是在MicroMassIsoprobe型MC-ICP-MS仪器上完成的,该仪器配有9个法拉第杯、4个粒子计数信道和1个电子倍增器共14个接收器.详细的实验流程参见有关文献(韦刚健等,2002;梁细荣等,2003).

2.3 电子探针分析

电子探针分析在西北大学大陆动力学国家重点实验室JEOL JXA-8230型电子探针仪上完成.其实验条件为:加速电压为15 kV,电流为20 nA,束斑直径通常为1 μm.矿物标样由SPI公司提供,不同矿物标样用于校正不同元素,硬玉校正Si、Al、Na,透辉石-Ca,橄榄石-Mg,透长石-K,钛铁矿-Fe,蔷薇辉石-Mn,金红石-Ti.

3 分析结果

3.1 LA-ICP-MS锆石U-Pb年代学

对阳江市八二花岗质岩体的1件MMEs样品(15YD-01)和1件寄主岩样品(15YD-02)进行了锆

石U-Pb年代学分析,相关的同位素比值和年龄结果见表1.MMEs和寄主岩所选锆石晶型较好,颗粒较大,锆石形态完整,具清晰的韵律振荡环带结构,是典型的岩浆锆石(Whitehouse and Platt, 2003; 吴元保和郑永飞, 2004),因此所获得的年龄可以代表岩石的结晶年龄.在年龄谐和图上,MMEs中的点04、06、11以及寄主岩中的点13谐和度较低(表1),在计算加权平均年龄时将它们剔除,其余数据谐和度较好,样品点均位于谐和线上及其附近.对寄主岩样品所测定的24颗锆石样品的 $^{206}\text{Pb}/^{238}\text{U}$ 加权平均年龄为 160.0 ± 1.0 Ma (MSWD=0.1, 图4a),对MMEs样品所测定的22颗锆石样品的 $^{206}\text{Pb}/^{238}\text{U}$ 加权平均年龄为 159.3 ± 1.1 Ma (MSWD=0.3, 图4b).

3.2 主量及微量元素

本文分别选取了八二花岗质岩体的5件寄主岩和5件MMEs进行全岩主量元素和微量元素测试,其结果见表2.同时引用邻区小梁和岗尾岩体(159~165 Ma)中高钾钙碱性I型花岗岩(王岳军等,2004; Huang *et al.*, 2013)的地球化学数据作为对比.

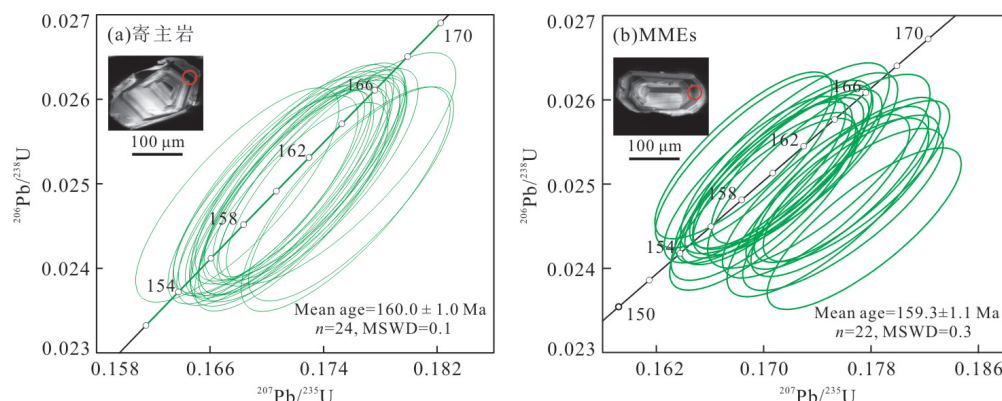


图4 寄主岩(a)和MMEs(b)的锆石U-Pb年龄谐和图

Fig.4 Zircon U-Pb concordia diagrams of host rocks (a) and mafic microgranular enclaves (b) from the Ba'er pluton

表1 暗色微粒包体及寄主岩锆石LA-MC-ICP-MS锆石U-Pb定年结果

Table 1 LA-MC-ICP-MS U-Pb zircon data of host rocks and MMEs in the Ba'er pluton

| 样品 | 同位素比值 | | | | | | 年龄(Ma) | | | | | | |
|------------|-----------------------------------|-----------|----------------------------------|-----------|----------------------------------|-----------|-----------------------------------|-----------|----------------------------------|-----------|----------------------------------|-----------|-----|
| | $^{207}\text{Pb}/^{206}\text{Pb}$ | 1σ | $^{207}\text{Pb}/^{235}\text{U}$ | 1σ | $^{206}\text{Pb}/^{238}\text{U}$ | 1σ | $^{207}\text{Pb}/^{206}\text{Pb}$ | 1σ | $^{207}\text{Pb}/^{235}\text{U}$ | 1σ | $^{206}\text{Pb}/^{238}\text{U}$ | 1σ | 谐和度 |
| 暗色微粒包体 | | | | | | | | | | | | | |
| 15YD-01-01 | 0.048 75 | 0.001 73 | 0.171 43 | 0.005 48 | 0.025 20 | 0.000 80 | 200 | 83 | 161 | 5 | 160 | 5 | 99% |
| 15YD-01-02 | 0.048 44 | 0.001 68 | 0.169 34 | 0.005 52 | 0.025 05 | 0.000 81 | 121 | 88 | 159 | 5 | 160 | 5 | 99% |
| 15YD-01-03 | 0.050 57 | 0.001 73 | 0.175 49 | 0.005 56 | 0.024 96 | 0.000 79 | 220 | 80 | 164 | 5 | 159 | 5 | 96% |
| 15YD-01-04 | 0.062 78 | 0.002 16 | 0.235 91 | 0.008 60 | 0.027 07 | 0.000 89 | 702 | 69 | 215 | 7 | 172 | 6 | 77% |
| 15YD-01-05 | 0.048 68 | 0.001 59 | 0.171 59 | 0.006 36 | 0.025 31 | 0.000 93 | 132 | 76 | 161 | 6 | 161 | 6 | 99% |

续表1

| 样品 | 同位素比值 | | | | | | 年龄(Ma) | | | | | | |
|------------|-----------------------------------|-----------|----------------------------------|-----------|----------------------------------|-----------|-----------------------------------|-----------|----------------------------------|-----------|----------------------------------|-----------|-----|
| | $^{207}\text{Pb}/^{206}\text{Pb}$ | 1σ | $^{207}\text{Pb}/^{235}\text{U}$ | 1σ | $^{206}\text{Pb}/^{238}\text{U}$ | 1σ | $^{207}\text{Pb}/^{206}\text{Pb}$ | 1σ | $^{207}\text{Pb}/^{235}\text{U}$ | 1σ | $^{206}\text{Pb}/^{238}\text{U}$ | 1σ | 谐和度 |
| 15YD-01-06 | 0.056 48 | 0.002 00 | 0.195 18 | 0.007 86 | 0.024 54 | 0.000 87 | 472 | 78 | 181 | 7 | 156 | 6 | 85% |
| 15YD-01-07 | 0.049 12 | 0.001 57 | 0.170 61 | 0.005 59 | 0.025 03 | 0.000 81 | 154 | 79 | 160 | 5 | 159 | 5 | 99% |
| 15YD-01-08 | 0.050 64 | 0.001 57 | 0.176 22 | 0.005 67 | 0.025 05 | 0.000 80 | 233 | 72 | 165 | 5 | 160 | 5 | 96% |
| 15YD-01-09 | 0.048 92 | 0.001 50 | 0.171 27 | 0.005 54 | 0.025 24 | 0.000 81 | 143 | 68 | 161 | 5 | 161 | 5 | 99% |
| 15YD-01-10 | 0.049 35 | 0.001 51 | 0.173 05 | 0.005 67 | 0.025 31 | 0.000 83 | 165 | 68 | 162 | 5 | 161 | 5 | 99% |
| 15YD-01-11 | 0.055 85 | 0.001 72 | 0.236 32 | 0.007 67 | 0.030 77 | 0.001 02 | 456 | 73 | 215 | 6 | 195 | 6 | 90% |
| 15YD-01-12 | 0.049 60 | 0.001 50 | 0.170 01 | 0.005 74 | 0.024 76 | 0.000 83 | 176 | 75 | 159 | 5 | 158 | 5 | 98% |
| 15YD-01-13 | 0.049 52 | 0.001 51 | 0.169 98 | 0.005 62 | 0.024 85 | 0.000 81 | 172 | 72 | 159 | 5 | 158 | 5 | 99% |
| 15YD-01-14 | 0.051 21 | 0.001 54 | 0.174 78 | 0.006 14 | 0.024 72 | 0.000 87 | 250 | 64 | 164 | 5 | 157 | 6 | 96% |
| 15YD-01-15 | 0.050 77 | 0.001 58 | 0.173 91 | 0.005 70 | 0.024 86 | 0.000 79 | 232 | 68 | 163 | 5 | 158 | 5 | 97% |
| 15YD-01-16 | 0.051 46 | 0.001 63 | 0.176 06 | 0.005 72 | 0.024 86 | 0.000 78 | 261 | 72 | 165 | 5 | 158 | 5 | 96% |
| 15YD-01-17 | 0.052 49 | 0.001 60 | 0.177 49 | 0.005 91 | 0.024 47 | 0.000 78 | 306 | 70 | 166 | 5 | 156 | 5 | 93% |
| 15YD-01-18 | 0.048 62 | 0.001 50 | 0.168 70 | 0.005 52 | 0.025 26 | 0.000 83 | 128 | 79 | 158 | 5 | 161 | 5 | 98% |
| 15YD-01-19 | 0.048 39 | 0.001 48 | 0.168 50 | 0.005 39 | 0.025 34 | 0.000 81 | 117 | 72 | 158 | 5 | 161 | 5 | 97% |
| 15YD-01-20 | 0.051 52 | 0.001 63 | 0.175 91 | 0.006 10 | 0.024 70 | 0.000 79 | 265 | 77 | 165 | 5 | 157 | 5 | 95% |
| 15YD-01-21 | 0.049 32 | 0.001 50 | 0.170 00 | 0.005 39 | 0.025 02 | 0.000 78 | 165 | 66 | 159 | 5 | 159 | 5 | 99% |
| 15YD-01-22 | 0.050 12 | 0.001 55 | 0.174 11 | 0.006 77 | 0.025 15 | 0.000 94 | 211 | 103 | 163 | 6 | 160 | 6 | 98% |
| 15YD-01-23 | 0.051 20 | 0.001 57 | 0.176 91 | 0.005 67 | 0.025 04 | 0.000 78 | 250 | 72 | 165 | 5 | 159 | 5 | 96% |
| 15YD-01-24 | 0.049 35 | 0.001 52 | 0.170 99 | 0.005 61 | 0.025 09 | 0.000 79 | 165 | 68 | 160 | 5 | 160 | 5 | 99% |
| 15YD-01-25 | 0.049 51 | 0.001 55 | 0.171 77 | 0.005 75 | 0.025 14 | 0.000 81 | 172 | 72 | 161 | 5 | 160 | 5 | 99% |
| 寄主岩 | | | | | | | | | | | | | |
| 15YD-02-01 | 0.049 51 | 0.001 50 | 0.172 49 | 0.005 95 | 0.025 21 | 0.000 87 | 172 | 72 | 162 | 5 | 161 | 6 | 99% |
| 15YD-02-02 | 0.049 25 | 0.001 49 | 0.170 60 | 0.005 68 | 0.025 07 | 0.000 83 | 167 | 70 | 160 | 5 | 160 | 5 | 99% |
| 15YD-02-03 | 0.049 61 | 0.001 51 | 0.172 01 | 0.006 03 | 0.025 11 | 0.000 87 | 176 | 75 | 161 | 5 | 160 | 6 | 99% |
| 15YD-02-04 | 0.049 74 | 0.001 50 | 0.171 74 | 0.005 57 | 0.024 98 | 0.000 81 | 183 | 70 | 161 | 5 | 159 | 5 | 98% |
| 15YD-02-05 | 0.049 53 | 0.001 49 | 0.171 95 | 0.005 50 | 0.025 13 | 0.000 80 | 172 | 70 | 161 | 5 | 160 | 5 | 99% |
| 15YD-02-06 | 0.049 67 | 0.001 50 | 0.173 23 | 0.005 41 | 0.025 25 | 0.000 78 | 189 | 73 | 162 | 5 | 161 | 5 | 99% |
| 15YD-02-07 | 0.048 95 | 0.001 49 | 0.170 42 | 0.005 71 | 0.025 19 | 0.000 84 | 146 | 72 | 160 | 5 | 160 | 5 | 99% |
| 15YD-02-08 | 0.049 65 | 0.001 52 | 0.175 23 | 0.006 61 | 0.025 35 | 0.000 90 | 189 | 75 | 164 | 6 | 161 | 6 | 98% |
| 15YD-02-09 | 0.050 96 | 0.001 54 | 0.175 56 | 0.006 02 | 0.025 05 | 0.000 87 | 239 | 69 | 164 | 5 | 160 | 6 | 97% |
| 15YD-02-10 | 0.049 54 | 0.001 49 | 0.173 01 | 0.005 56 | 0.025 31 | 0.000 81 | 172 | 70 | 162 | 5 | 161 | 5 | 99% |
| 15YD-02-11 | 0.049 24 | 0.001 51 | 0.170 56 | 0.005 55 | 0.025 11 | 0.000 80 | 167 | 70 | 160 | 5 | 160 | 5 | 99% |
| 15YD-02-12 | 0.049 42 | 0.001 49 | 0.171 24 | 0.005 71 | 0.025 14 | 0.000 84 | 169 | 70 | 161 | 5 | 160 | 5 | 99% |
| 15YD-02-13 | 0.059 55 | 0.001 89 | 0.201 13 | 0.007 03 | 0.024 45 | 0.000 81 | 587 | 69 | 186 | 6 | 156 | 5 | 82% |
| 15YD-02-14 | 0.049 14 | 0.001 49 | 0.170 14 | 0.005 52 | 0.025 13 | 0.000 81 | 154 | 75 | 160 | 5 | 160 | 5 | 99% |
| 15YD-02-15 | 0.049 67 | 0.001 56 | 0.172 44 | 0.005 68 | 0.025 23 | 0.000 80 | 189 | 72 | 162 | 5 | 161 | 5 | 99% |
| 15YD-02-16 | 0.049 50 | 0.001 49 | 0.172 66 | 0.005 76 | 0.025 32 | 0.000 84 | 172 | 70 | 162 | 5 | 161 | 5 | 99% |
| 15YD-02-17 | 0.048 88 | 0.001 62 | 0.167 92 | 0.005 85 | 0.025 09 | 0.000 83 | 143 | 78 | 158 | 5 | 160 | 5 | 98% |
| 15YD-02-18 | 0.049 98 | 0.001 52 | 0.173 58 | 0.005 80 | 0.025 26 | 0.000 84 | 195 | 72 | 163 | 5 | 161 | 5 | 98% |
| 15YD-02-19 | 0.049 24 | 0.001 48 | 0.169 73 | 0.005 47 | 0.025 05 | 0.000 81 | 167 | 70 | 159 | 5 | 160 | 5 | 99% |
| 15YD-02-20 | 0.049 38 | 0.001 49 | 0.171 95 | 0.005 72 | 0.025 30 | 0.000 84 | 165 | 68 | 161 | 5 | 161 | 5 | 99% |
| 15YD-02-21 | 0.049 65 | 0.001 50 | 0.171 56 | 0.005 70 | 0.025 09 | 0.000 82 | 189 | 75 | 161 | 5 | 160 | 5 | 99% |
| 15YD-02-22 | 0.049 56 | 0.001 50 | 0.171 71 | 0.005 86 | 0.025 18 | 0.000 85 | 176 | 70 | 161 | 5 | 160 | 5 | 99% |
| 15YD-02-23 | 0.050 87 | 0.001 56 | 0.175 94 | 0.005 91 | 0.025 10 | 0.000 83 | 235 | 72 | 165 | 5 | 160 | 5 | 97% |
| 15YD-02-24 | 0.049 24 | 0.001 49 | 0.171 56 | 0.005 61 | 0.025 26 | 0.000 82 | 167 | 70 | 161 | 5 | 161 | 5 | 99% |
| 15YD-02-25 | 0.049 77 | 0.001 51 | 0.172 53 | 0.006 02 | 0.025 16 | 0.000 88 | 183 | 66 | 162 | 5 | 160 | 6 | 99% |

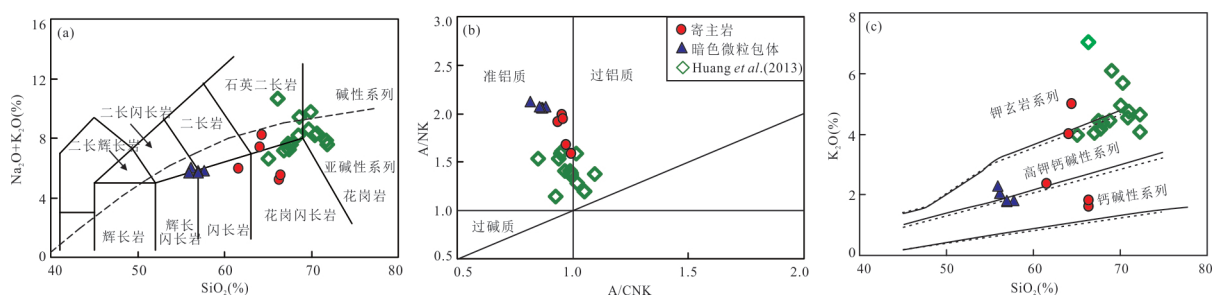
表 2 暗色微粒包体及寄主岩主量元素(%)、微量元素(10^{-6})和 Sr-Nd 同位素组成分析结果Table 2 Major oxides (%), trace elements (10^{-6}) and Sr-Nd isotopic results of host rocks and MMEs in the Ba'er pluton

| 样品 | YD-01C | YD-01D | YD-01E | YD-01F | YD-01G | YD-02A | YD-02B | YD-02C | YD-02D | YD-02E |
|--------------------------------|--------|--------|--------|--------|--------|--------|---------|--------|--------|--------|
| 岩性 | 暗色微粒包体 | | | | | | 寄主岩 | | | |
| SiO ₂ | 55.53 | 57.08 | 56.44 | 55.26 | 56.42 | 65.84 | 63.94 | 61.04 | 65.98 | 63.73 |
| TiO ₂ | 1.29 | 1.16 | 1.22 | 1.12 | 1.25 | 0.74 | 0.55 | 0.98 | 0.72 | 0.66 |
| Al ₂ O ₃ | 17.83 | 17.36 | 17.37 | 16.83 | 17.23 | 15.10 | 16.81 | 16.07 | 15.47 | 16.34 |
| CaO | 6.50 | 6.18 | 6.42 | 6.99 | 6.50 | 4.54 | 3.47 | 4.81 | 4.52 | 3.87 |
| FeO _t | 8.68 | 8.15 | 8.46 | 8.54 | 8.55 | 5.69 | 4.62 | 7.41 | 5.28 | 5.42 |
| K ₂ O | 2.04 | 1.79 | 1.80 | 2.25 | 1.76 | 1.60 | 4.97 | 2.34 | 1.79 | 3.97 |
| MgO | 2.79 | 2.84 | 2.96 | 4.02 | 2.98 | 1.85 | 1.51 | 2.45 | 1.68 | 1.71 |
| MnO | 0.14 | 0.16 | 0.16 | 0.21 | 0.17 | 0.11 | 0.09 | 0.14 | 0.10 | 0.10 |
| Na ₂ O | 3.91 | 3.93 | 3.93 | 3.33 | 3.90 | 3.56 | 3.17 | 3.56 | 3.66 | 3.34 |
| P ₂ O ₅ | 0.29 | 0.27 | 0.30 | 0.27 | 0.30 | 0.23 | 0.18 | 0.30 | 0.21 | 0.21 |
| LOI | 0.70 | 0.79 | 0.64 | 0.89 | 0.66 | 0.49 | 0.41 | 0.61 | 0.33 | 0.37 |
| Total | 99.70 | 99.71 | 99.70 | 99.70 | 99.70 | 99.73 | 99.72 | 99.72 | 99.73 | 99.72 |
| Mg [#] | 43 | 45 | 45 | 52 | 45 | 43 | 43 | 43 | 43 | 42 |
| A/CNK | 0.87 | 0.88 | 0.86 | 0.82 | 0.86 | 0.95 | 1.00 | 0.94 | 0.96 | 0.97 |
| A/NK | 2.06 | 2.07 | 2.06 | 2.13 | 2.07 | 1.99 | 1.59 | 1.91 | 1.95 | 1.67 |
| Li | 85.01 | 91.64 | 88.74 | 75.77 | 82.12 | 77.96 | 60.77 | 95.46 | 64.63 | 61.73 |
| Be | 2.28 | 2.29 | 3.11 | 3.90 | 2.41 | 4.02 | 3.64 | 4.17 | 3.86 | 3.98 |
| Sc | 20.23 | 18.79 | 21.05 | 22.12 | 19.19 | 13.01 | 11.32 | 16.69 | 12.36 | 12.67 |
| V | 214.08 | 186.56 | 192.97 | 189.19 | 193.03 | 100.51 | 85.71 | 129.97 | 95.80 | 97.29 |
| Cr | 11.31 | 12.41 | 7.26 | 34.95 | 8.09 | 13.23 | 16.95 | 20.55 | 10.37 | 11.47 |
| Co | 22.67 | 22.00 | 21.59 | 24.81 | 22.17 | 12.57 | 9.74 | 16.57 | 11.68 | 11.57 |
| Ni | 6.60 | 7.64 | 6.34 | 17.83 | 6.57 | 6.25 | 5.51 | 13.64 | 5.45 | 4.82 |
| Cu | 21.38 | 28.47 | 27.31 | 28.20 | 28.68 | 11.03 | 6.56 | 12.16 | 6.68 | 7.13 |
| Zn | 145.90 | 143.76 | 144.54 | 133.97 | 138.40 | 97.36 | 82.46 | 123.55 | 88.49 | 87.27 |
| Ga | 21.94 | 21.40 | 21.01 | 20.86 | 20.80 | 19.81 | 17.66 | 21.02 | 19.40 | 18.30 |
| Rb | 127.99 | 149.81 | 145.66 | 120.19 | 138.23 | 113.00 | 167.92 | 158.16 | 119.28 | 163.05 |
| Sr | 516.70 | 440.97 | 446.41 | 428.97 | 441.45 | 383.59 | 445.22 | 390.81 | 397.78 | 431.19 |
| Y | 31.06 | 27.91 | 29.88 | 33.07 | 31.34 | 27.31 | 16.68 | 32.46 | 27.77 | 21.26 |
| Zr | 231.07 | 222.79 | 198.25 | 163.96 | 210.34 | 234.43 | 201.91 | 303.35 | 212.46 | 207.94 |
| Nb | 13.67 | 13.00 | 14.33 | 16.70 | 14.61 | 15.02 | 9.63 | 18.94 | 14.76 | 12.07 |
| Cs | 9.34 | 11.82 | 11.30 | 6.88 | 11.26 | 8.01 | 8.33 | 11.15 | 9.36 | 9.70 |
| Ba | 538.47 | 240.85 | 316.04 | 461.07 | 253.69 | 150.31 | 1064.07 | 284.51 | 200.39 | 720.25 |
| La | 38.32 | 45.51 | 45.36 | 27.14 | 42.23 | 60.87 | 32.81 | 47.87 | 40.86 | 39.56 |
| Ce | 77.87 | 84.96 | 87.67 | 61.15 | 85.01 | 109.52 | 61.45 | 95.27 | 76.19 | 70.96 |
| Pr | 9.24 | 9.16 | 10.03 | 7.46 | 9.84 | 11.36 | 6.26 | 10.72 | 8.51 | 7.66 |
| Nd | 34.37 | 34.09 | 36.49 | 30.41 | 37.33 | 37.30 | 21.95 | 38.62 | 29.75 | 24.74 |
| Sm | 6.86 | 6.00 | 7.10 | 6.62 | 7.19 | 6.71 | 3.57 | 6.98 | 5.78 | 4.67 |
| Eu | 1.70 | 1.49 | 1.70 | 1.48 | 1.70 | 1.37 | 0.91 | 1.61 | 1.29 | 1.06 |
| Gd | 6.54 | 5.98 | 6.70 | 6.51 | 6.73 | 5.99 | 3.30 | 6.69 | 5.32 | 3.72 |
| Tb | 0.97 | 0.90 | 0.99 | 0.96 | 1.03 | 0.92 | 0.50 | 1.03 | 0.82 | 0.63 |
| Dy | 5.19 | 4.74 | 5.30 | 5.49 | 5.50 | 4.59 | 2.61 | 5.78 | 4.38 | 3.21 |
| Ho | 1.01 | 0.90 | 1.03 | 1.08 | 1.06 | 0.92 | 0.56 | 1.12 | 0.87 | 0.62 |
| Er | 2.89 | 2.65 | 2.92 | 3.16 | 2.97 | 2.69 | 1.58 | 3.16 | 2.50 | 1.95 |
| Tm | 0.41 | 0.35 | 0.40 | 0.46 | 0.40 | 0.39 | 0.23 | 0.46 | 0.35 | 0.28 |
| Yb | 2.53 | 2.22 | 2.56 | 3.05 | 2.64 | 2.47 | 1.49 | 3.02 | 2.38 | 1.83 |
| Lu | 0.38 | 0.34 | 0.40 | 0.45 | 0.39 | 0.39 | 0.24 | 0.45 | 0.36 | 0.30 |

续表2

| 样品 | YD-01C | YD-01D | YD-01E | YD-01F | YD-01G | YD-02A | YD-02B | YD-02C | YD-02D | YD-02E |
|-------------------------------------|-----------|--------|--------|-----------|--------|-----------|--------|--------|-----------|--------|
| Hf | 5.21 | 5.02 | 4.74 | 3.88 | 5.11 | 5.90 | 4.93 | 7.68 | 4.89 | 4.80 |
| Ta | 0.80 | 0.75 | 0.95 | 0.85 | 1.26 | 1.77 | 0.95 | 2.02 | 1.69 | 1.16 |
| W | 1.04 | 0.86 | 0.73 | 1.13 | 1.42 | 0.50 | 0.77 | 1.13 | 0.66 | 0.51 |
| Tl | 0.64 | 0.76 | 0.77 | 0.60 | 0.76 | 0.61 | 0.84 | 0.88 | 0.59 | 0.76 |
| Pb | 12.92 | 14.15 | 14.65 | 12.71 | 14.77 | 14.00 | 26.35 | 14.71 | 13.48 | 19.56 |
| Bi | 0.21 | 0.25 | 0.26 | 0.19 | 0.23 | 0.24 | 0.18 | 0.22 | 0.22 | 0.19 |
| Th | 8.82 | 10.92 | 10.70 | 6.77 | 10.35 | 25.51 | 16.23 | 22.35 | 17.88 | 16.96 |
| U | 2.06 | 2.54 | 2.77 | 1.93 | 2.46 | 6.35 | 4.60 | 6.72 | 5.25 | 4.77 |
| Eu* | 0.78 | 0.76 | 0.75 | 0.69 | 0.75 | 0.66 | 0.81 | 0.72 | 0.71 | 0.78 |
| $T_{\text{z}}(\text{°C})$ | | | | | | 746 | 732 | 754 | 737 | 730 |
| ΣREE | 188.28 | 199.29 | 208.66 | 155.41 | 204.01 | 245.49 | 137.46 | 222.78 | 179.34 | 161.20 |
| LREE | 168.35 | 181.21 | 188.36 | 134.27 | 183.29 | 227.13 | 126.96 | 201.07 | 162.37 | 148.65 |
| HREE | 19.92 | 18.07 | 20.30 | 21.14 | 20.71 | 18.36 | 10.50 | 21.71 | 16.97 | 12.55 |
| LREE/HREE | 8.45 | 10.03 | 9.28 | 6.35 | 8.85 | 12.37 | 12.09 | 9.26 | 9.57 | 11.85 |
| (La/Yb) _N | 10.85 | 14.73 | 12.70 | 6.39 | 11.47 | 17.67 | 15.80 | 11.38 | 12.29 | 15.47 |
| Rb/Sr | 0.25 | 0.34 | 0.33 | 0.28 | 0.31 | 0.29 | 0.38 | 0.40 | 0.30 | 0.38 |
| Nb/Ta | 17.2 | 17.3 | 15.0 | 19.7 | 11.6 | 8.5 | 10.1 | 9.4 | 8.7 | 10.4 |
| $^{87}\text{Rb}/^{86}\text{Sr}$ | 0.436 34 | | | 0.983 16 | | 0.852 46 | | | 0.867 79 | |
| $^{147}\text{Sm}/^{144}\text{Nd}$ | 0.100 26 | | | 0.106 47 | | 0.108 69 | | | 0.117 38 | |
| $^{87}\text{Sr}/^{86}\text{Sr}$ | 0.708 02 | | | 0.709 93 | | 0.709 54 | | | 0.709 60 | |
| 2σ | 0.000 008 | | | 0.000 008 | | 0.000 006 | | | 0.000 006 | |
| $^{143}\text{Nd}/^{144}\text{Nd}$ | 0.512 316 | | | 0.512 247 | | 0.512 254 | | | 0.512 266 | |
| 2σ | 0.000 006 | | | 0.000 005 | | 0.000 003 | | | 0.000 006 | |
| $(^{87}\text{Sr}/^{86}\text{Sr})_i$ | 0.707 04 | | | 0.707 74 | | 0.707 63 | | | 0.707 67 | |
| $\epsilon_{\text{Nd}}(t)$ | -4.35 | | | -5.81 | | -5.73 | | | -5.67 | |
| $T_{\text{DM}}^2 (\text{Ga})$ | 1.12 | | | 1.28 | | 1.30 | | | 1.40 | |

注: LOI, 烧失量; A/NK(摩尔比) = $\text{Al}_2\text{O}_3/(\text{Na}_2\text{O} + \text{K}_2\text{O})$; A/CNK(摩尔比) = $\text{Al}_2\text{O}_3/(\text{Na}_2\text{O} + \text{K}_2\text{O} + \text{CaO})$; Eu* = $\text{Eu}_{\text{N}}/[(\text{Sm}_{\text{N}} \times \text{Gd}_{\text{N}})^{1/2}]$; $(^{87}\text{Sr}/^{86}\text{Sr})_i = (^{87}\text{Sr}/^{86}\text{Sr})_s - (^{87}\text{Rb}/^{86}\text{Sr})_s \times (e^{\lambda t} - 1)$; $\lambda = 1.42 \times 10^{-11} \text{ a}^{-1}$; $\epsilon_{\text{Sr}} = [(\text{Nd}_{\text{S}}/^{144}\text{Nd})_{\text{CHUR}} - 1] \times 10000$; $\epsilon_{\text{Nd}} = [(\text{Nd}_{\text{S}}/^{144}\text{Nd})_{\text{CHUR}} - 1] \times 10000$; t 代表样品形成时间, S代表样品, CHUR代表球粒陨石; $(^{147}\text{Sm}/^{144}\text{Nd})_{\text{CHUR}} = 0.1967$; $(^{143}\text{Nd}/^{144}\text{Nd})_{\text{CHUR}} = 0.512638$

图5 寄主岩和MMEs的TAS(a)、A/CNK-A/NK(b)和SiO₂-K₂O(c)图解Fig.5 TAS (a), A/CNK-A/NK(b) and SiO₂-K₂O(c) classification diagrams for the Ba'er pluton

图b据Maniar and Piccoli(1989);图c据Rickwood(1989)

3.2.1 寄主岩主量及微量元素特征 八二花岗质岩体中寄主岩SiO₂含量变化范围较窄(61.04%~65.84%), 在TAS分类图解中(图5a), 寄主岩样品主要落入亚碱性系列中的石英二长岩和花岗闪长岩范畴。TiO₂含量介于0.55%~0.98%, CaO含量为

3.47%~4.81%, Al₂O₃含量介于15.10%~16.81%, 铝饱和指数A/CNK在0.94~1.00之间(平均值为0.96), A/NK为1.59~1.99, 属于准铝质系列花岗岩, 与邻区的同时代小梁、岗尾岩体特征相似(图5b, Huang et al., 2013)。全碱含量为(5.16%~

8.14%), K_2O 为 1.60%~4.97%, K_2O/Na_2O 比值介于 0.45~1.57, 里特曼指数(σ)在 0.99~3.46 之间, 在 K_2O-SiO_2 图解中, 寄主岩样品点分布较分散, 从钙碱性系列到钾玄岩系列均有分布(图 5c). MgO 含量介于 1.51%~2.45%, 平均值为 1.84%, 其 $Mg^{\#}$ =42~43 均小于 45, 接近典型壳源熔体的镁指数(Rapp and Watson, 1995).

寄主岩稀土元素(表 2)总量较高(137×10^{-6} ~ 245×10^{-6} , 平均为 189×10^{-6}); 轻稀土总量在 127×10^{-6} ~ 227×10^{-6} 之间, 重稀土总量为 10.5×10^{-6} ~ 18.4×10^{-6} , 轻、重稀土元素之间分馏较明显. (La/Yb)_N 为 11.4~17.7, 平均为 14.5. 在稀土元素配分图上(图 6a)显示为右倾型, 重稀土的曲线型式比较平坦, 与典型 S 型花岗岩表现出的“海鸥型”稀土元素配分型式有较大差别. 样品具弱一中等的负 Eu 异常, δEu 为 0.66~0.81, 平均为 0.73. 在原始地幔标准化微量元素蛛网图上(图 6b), 寄主岩富集 Rb、Th 和 U 等大离子亲石元素, 亏损 Nb、Ta 和 Ti 等高场强元素.

3.2.2 MMEs 主量及微量元素特征

八二花岗质岩体中 MMEs 的主量元素(表 2)具有如下特征: MMEs 的 SiO_2 含量比较低, 含量介于 55.26%~

57.08%, 属于闪长质, 在 TAS 分类图解中(图 5a), MMEs 主要位于闪长岩、辉长闪长岩和二长闪长岩的界限附近. CaO 含量为 6.18%~6.99%, Al_2O_3 含量介于 16.83%~17.83%, 平均为 17.33%, 高于寄主岩, 铝饱和指数 A/CNK 介于 0.82~0.88, 平均值为 0.86, 属于准铝质系列(图 5b). 全碱含量介于 5.58%~5.95%, 略低于寄主岩, K_2O/Na_2O 比值介于 0.45~0.68, 里特曼指数(σ)为 1.93~2.99, K_2O 为 1.76%~2.25%, 在 K_2O-SiO_2 图解中(图 5c), MMEs 样品分布相对集中, 分布在钙碱性—高钾钙碱性系列; MgO 含量介于 2.79%~4.02%, 平均值为 3.13%, 其 $Mg^{\#}$ =43~52, 略高于寄主岩. 在 Harker 图解(图 7)中, 寄主岩石与 MMEs 的主量元素具有较好的线性演化趋势关系, 随着 SiO_2 的增加, Al_2O_3 、 CaO 、 P_2O_5 、 MgO 、 TiO_2 、 $FeOt$ 呈线性降低, 反映其经历了斜长石、磷灰石及钛铁矿等矿物的分离结晶作用(李献华等, 2000).

MMEs 与寄主岩相比, 稀土元素总量基本相当(155×10^{-6} ~ 209×10^{-6} , 平均为 191×10^{-6}). 轻、重稀土元素之间分馏较明显, (La/Yb)_N 为 6.4~14.7, 平均为 11.2. 在稀土元素配分图(图 6c)上也显示出与寄主岩的配分曲线相似的特征, 为右倾型, 重稀

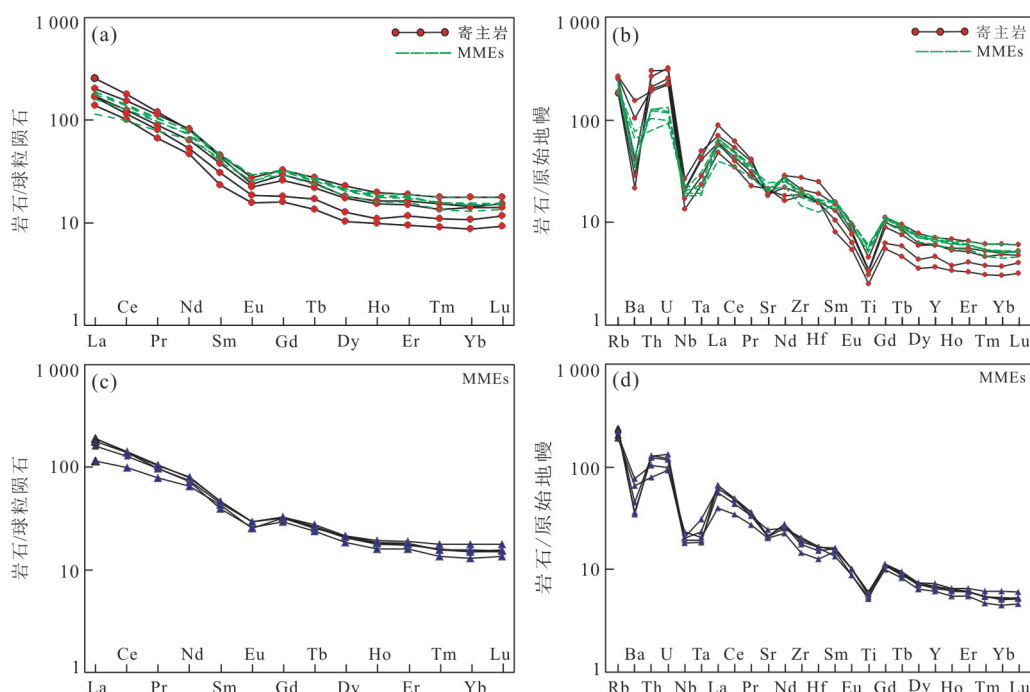


图 6 寄主岩(a,b)和 MMEs(c,d)的球粒陨石标准化稀土元素配分图、原始地幔标准化微量元素蛛网图

Fig.6 Chondrite-normalized REE patterns and primitive mantle-normalized spidergrams of host rocks (a, b) and mafic micro-granular enclaves (c, d)

球粒陨石、原始地幔数据引自 Sun and McDonough (1989)

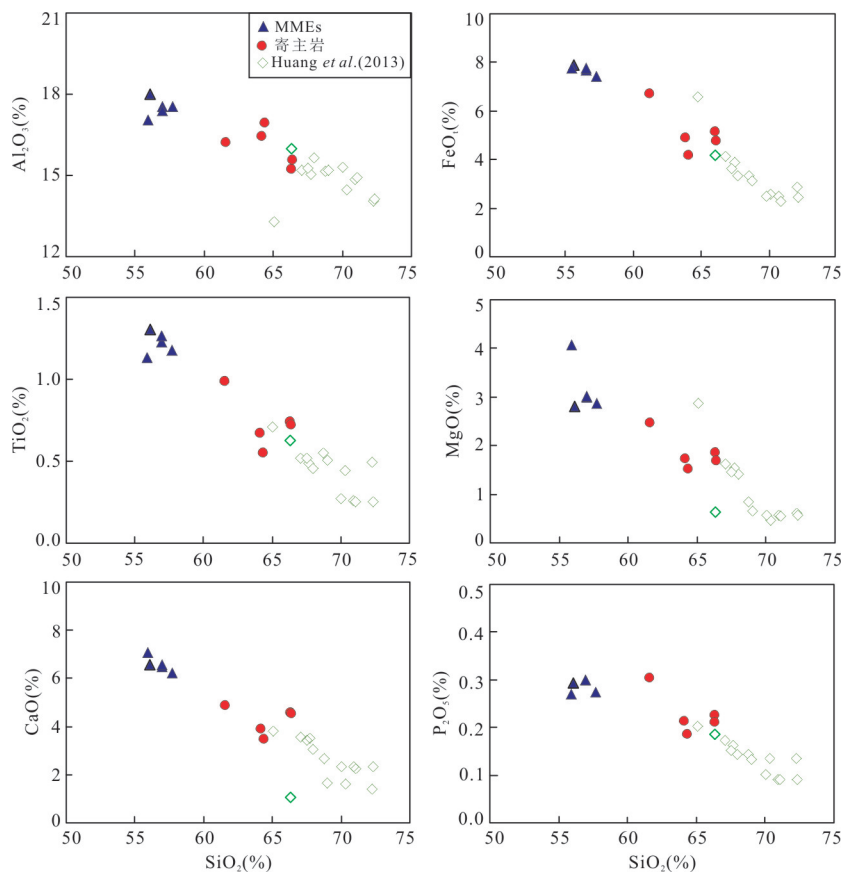


图7 寄主岩和MMEs的哈克图解
Fig.7 Harker diagrams of host granitoids and mafic microgranular enclaves

土分配模式比较平坦.Eu具有弱—中等的负异常, δEu 为0.69~0.78,平均为0.75,表明其形成过程中可能经历了斜长石的分离结晶作用.MMEs中Eu含量较寄主岩高(表2和图6),这可能是因为Eu主要以类质同象的形式赋存在斜长石里,在岩浆混合的过程中,MMEs捕获寄主岩中的斜长石从而使MMEs中含量较高,野外观察到MMEs中发育的斜长石斑晶也说明了这一点(图2d).

MMEs具有与寄主岩相似的微量元素组成,均表现出富集Rb、Th和U等大离子亲石元素,亏损Nb、Ta和Ti等高场强元素(图6d).MMEs的Rb/Sr比值为0.25~0.34.通过对MMEs和寄主岩的化学成分分析看出,MMEs和寄主岩的微量元素蛛网图分布具有很大的关联性,而且两者之间的主量元素也具有较好的线性相关性(图7),与Huang *et al.*(2013)报道的邻区小梁和岗尾岩体(159~165 Ma)具有相同的演化趋势.

3.3 矿物化学成分特征

寄主岩及MMEs中斜长石和角闪石的电子探针分析结果见表3和表4.MMEs和寄主岩中斜长石的

Na_2O 分别为6.60%~8.30%和6.83%~8.16%, K_2O 分别为0.11%~0.23%和0.07%~0.19%, CaO 分别为6.41%~8.83%和6.39%~8.37%.MMEs和寄主岩的斜长石均属于中长石的范畴,且两者的斜长石牌号An相似,MMEs为 $\text{An}_{30} \sim \text{An}_{42}$,寄主岩为 $\text{An}_{30} \sim \text{An}_{40}$.图8中的AB和CD均是两条横穿整个斜长石颗粒的剖面,可以看出,寄主岩和MMEs中的斜长石具有极为相似的化学组成,并且MMEs环带斜长石核部的An值略高于寄主岩斜长石核部的An值(图8).在寄主岩和MMEs中,部分斜长石具有清晰的环带结构,从核部到边部成分由较为基性的斜长石向酸性斜长石渐变,其An具有逐渐下降的变化趋势,为正环带结构.在岩浆温度快速下降的过程中,由于不断晶出的斜长石来不及与岩浆发生充分反应,就会被后来晶出的含An值较低、Ab值较高的斜长石成分所包裹,从而形成核部以An组分为主、边部以Ab组分为主的斜长石正常环带(图8;谢磊等,2004).当然环带结构本身也体现了结晶环境的动荡变化,指示了成岩过程可能伴随着一定程度的岩浆混合和分异过程(王德滋和谢磊,2008).

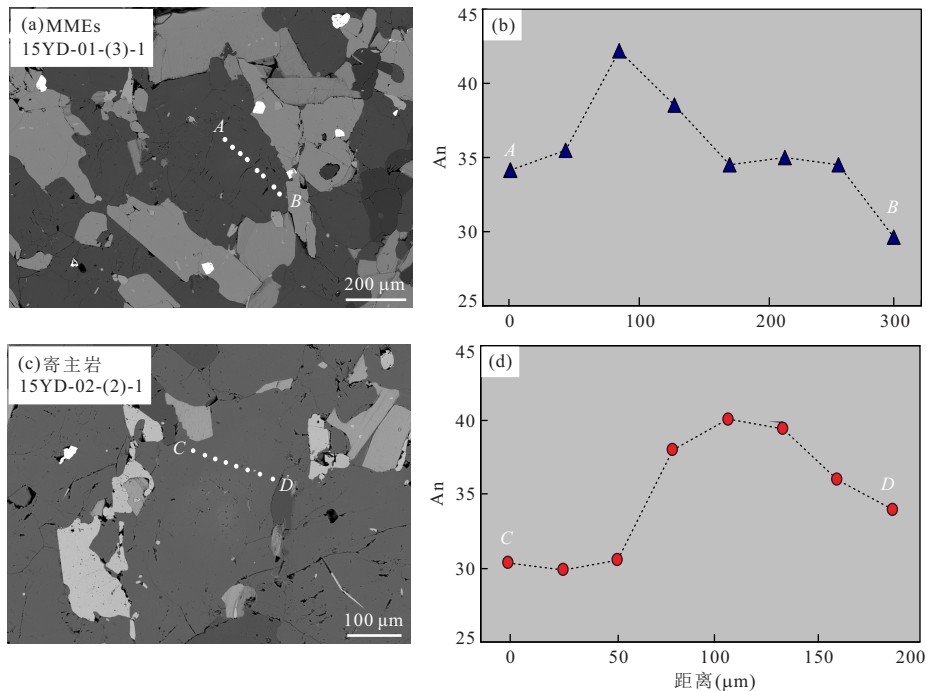


图8 MMEs中环带斜长石的背散射图像(a)和电子探针数据(b);寄主岩中环带斜长石的背散射图像(c)和电子探针数据(d)
Fig.8 Back-scattered electron images of zoned plagioclases (a, c) and EPMA data of the plagioclase component (b, d) of host rocks and MMEs, respectively

An为钙长石牌号

中酸性岩中的铁镁质矿物(如黑云母、角闪石等)往往蕴含着母岩浆成因的丰富信息,通过电子探针分析新鲜未遭蚀变、符合压力计矿物共生组合关系的角闪石,对探讨MMEs的形成来源以及成岩过程中的物理化学条件(如温度、压力等)等方面具有重要的指示意义(Lalonde and Bernard, 1993).本文选取MMEs和寄主岩中有代表性的角闪石进行电子探针测试分析,结果见表4.从数据可以看出,MMEs和寄主岩中角闪石的化学成分较为相似,均相对贫硅($\text{SiO}_2=41.99\% \sim 42.41\%$),富铁($\text{FeO}=20.22\% \sim 21.28\%$),所有角闪石均属于钙质角闪石系列(($\text{Ca}+\text{Na}$) B $\geqslant 1.00$, $\text{NaB}<0.50$; Leake, 1997).

3.4 Sr-Nd 同位素特征

MMEs及其寄主岩的Sr-Nd同位素组成如表2所示.MMEs的 $\epsilon_{\text{Nd}}(t)$ 值为 $-5.81 \sim -4.35$, $T_{\text{DM}}^2(\text{Nd})$ 为 $1.12 \sim 1.28$ Ga, $(^{87}\text{Sr}/^{86}\text{Sr})_i$ 值为 $0.707\ 04 \sim 0.707\ 74$;寄主岩的 $\epsilon_{\text{Nd}}(t)$ 值为 $-5.73 \sim -5.67$, $T_{\text{DM}}^2(\text{Nd})$ 为 $1.30 \sim 1.40$ Ga, $(^{87}\text{Sr}/^{86}\text{Sr})_i$ 值为 $0.707\ 63 \sim 0.707\ 67$.从图9可以看出,寄主岩和MMEs的Sr-Nd同位素组成基本一致,也与Huang

et al.(2013)研究的邻区同时代花岗岩同位素组成相近.

4 讨论

4.1 结晶温度和成岩压力

花岗岩类的成岩温度可以通过实验岩石学方法获得,也可以通过地质温度计方法进行估算.花岗质岩石大多是绝热上升侵位的,在这个过程中温度变化慢,所以岩浆早期结晶时的温度可以近似代表岩浆起源时的温度(吴福元等, 2008).为了进一步确定八二花岗质岩体成岩的物理化学条件,本文采用Boehnke et al.(2013)提出的锆石饱和温度计算公式,得到寄主岩的锆石饱和温度为 $730 \sim 754$ °C(表2),平均 740 °C($n=5$),相较于A型花岗岩的锆石饱和温度偏低(通常高于 800 °C).同时利用角闪石电子探针分析结果(表4),根据其温度选用Schmidt(1992)的角闪石全铝压力计($P(\pm 0.6 \times 10^8 \text{ Pa}) = -3.01 + 4.76 \text{ Al}^T$)对寄主岩及MMEs进行估算(表4),结果表明寄主岩角闪石的结晶压力变化于 $6.16 \times 10^8 \sim 6.34 \times 10^8$ Pa,平均压力为 6.25×10^8 Pa,MMEs中角闪石结晶时的压力范围

表 3 暗色微粒包体和寄主岩中斜长石的电子探针数据(%)

Table 3 EMPA results (%) of plagioclases in MMEs and host rocks

| Samples | SiO ₂ | TiO ₂ | Al ₂ O ₃ | FeO | MnO | MgO | CaO | Na ₂ O | K ₂ O | Total | Si | Al | Ca | Na | K | Or | Ab | An |
|-------------|------------------|------------------|--------------------------------|------|------|------|------|-------------------|------------------|--------|------|------|------|------|------|------|-------|-------|
| 暗色微粒包体 | | | | | | | | | | | | | | | | | | |
| 15YD-01-2-1 | 59.54 | 0.00 | 25.10 | 0.08 | 0.00 | 0.00 | 6.91 | 7.69 | 0.14 | 99.47 | 2.67 | 1.33 | 0.33 | 0.67 | 0.01 | 0.80 | 66.28 | 32.91 |
| 15YD-01-2-2 | 59.30 | 0.00 | 24.64 | 0.16 | 0.04 | 0.00 | 7.01 | 7.62 | 0.15 | 98.91 | 2.68 | 1.31 | 0.34 | 0.67 | 0.01 | 0.86 | 65.73 | 33.42 |
| 15YD-01-2-3 | 59.78 | 0.02 | 25.41 | 0.03 | 0.01 | 0.00 | 7.11 | 7.57 | 0.17 | 100.10 | 2.66 | 1.33 | 0.34 | 0.65 | 0.01 | 0.96 | 65.18 | 33.86 |
| 15YD-01-2-4 | 59.24 | 0.03 | 25.06 | 0.10 | 0.01 | 0.00 | 7.30 | 7.50 | 0.19 | 99.42 | 2.66 | 1.33 | 0.35 | 0.65 | 0.01 | 1.06 | 64.35 | 34.60 |
| 15YD-01-2-5 | 58.86 | 0.00 | 25.46 | 0.09 | 0.01 | 0.02 | 7.38 | 7.82 | 0.20 | 99.83 | 2.64 | 1.35 | 0.35 | 0.68 | 0.01 | 1.07 | 65.01 | 33.91 |
| 15YD-01-2-6 | 59.87 | 0.00 | 25.14 | 0.15 | 0.02 | 0.01 | 6.97 | 7.68 | 0.23 | 100.06 | 2.67 | 1.32 | 0.33 | 0.66 | 0.01 | 1.31 | 65.71 | 32.98 |
| 15YD-01-2-7 | 59.04 | 0.00 | 24.81 | 0.16 | 0.02 | 0.02 | 7.05 | 7.55 | 0.19 | 98.84 | 2.67 | 1.32 | 0.34 | 0.66 | 0.01 | 1.07 | 65.25 | 33.68 |
| 15YD-01-3-1 | 59.55 | 0.00 | 25.32 | 0.00 | 0.00 | 0.00 | 7.42 | 7.80 | 0.19 | 100.28 | 2.65 | 1.33 | 0.35 | 0.67 | 0.01 | 1.01 | 64.87 | 34.12 |
| 15YD-01-3-2 | 58.98 | 0.00 | 25.41 | 0.10 | 0.00 | 0.01 | 7.49 | 7.39 | 0.23 | 99.60 | 2.65 | 1.34 | 0.36 | 0.64 | 0.01 | 1.31 | 63.25 | 35.44 |
| 15YD-01-3-3 | 56.90 | 0.00 | 26.59 | 0.11 | 0.00 | 0.00 | 8.83 | 6.60 | 0.12 | 99.15 | 2.57 | 1.42 | 0.43 | 0.58 | 0.01 | 0.69 | 57.10 | 42.21 |
| 15YD-01-3-4 | 58.57 | 0.00 | 26.38 | 0.10 | 0.00 | 0.00 | 8.08 | 7.05 | 0.11 | 100.29 | 2.61 | 1.39 | 0.39 | 0.61 | 0.01 | 0.62 | 60.85 | 38.54 |
| 15YD-01-3-5 | 59.36 | 0.00 | 25.34 | 0.11 | 0.00 | 0.03 | 7.31 | 7.60 | 0.12 | 99.87 | 2.65 | 1.34 | 0.35 | 0.66 | 0.01 | 0.68 | 64.86 | 34.46 |
| 15YD-01-3-6 | 59.10 | 0.00 | 25.31 | 0.14 | 0.01 | 0.01 | 7.56 | 7.66 | 0.14 | 99.92 | 2.65 | 1.34 | 0.36 | 0.66 | 0.01 | 0.77 | 64.19 | 35.04 |
| 15YD-01-3-7 | 59.17 | 0.00 | 25.14 | 0.07 | 0.00 | 0.00 | 7.39 | 7.67 | 0.12 | 99.56 | 2.66 | 1.33 | 0.36 | 0.67 | 0.01 | 0.64 | 64.83 | 34.53 |
| 15YD-01-3-8 | 60.55 | 0.00 | 24.75 | 0.16 | 0.04 | 0.01 | 6.41 | 8.30 | 0.15 | 100.37 | 2.69 | 1.30 | 0.31 | 0.71 | 0.01 | 0.83 | 69.50 | 29.67 |
| 寄主岩 | | | | | | | | | | | | | | | | | | |
| 15YD-02-2-1 | 60.53 | 0.07 | 24.63 | 0.05 | 0.00 | 0.00 | 6.46 | 8.11 | 0.12 | 99.98 | 2.70 | 1.29 | 0.31 | 0.70 | 0.01 | 0.69 | 68.98 | 30.34 |
| 15YD-02-2-2 | 60.60 | 0.01 | 24.65 | 0.09 | 0.00 | 0.00 | 6.39 | 8.16 | 0.18 | 100.08 | 2.70 | 1.29 | 0.30 | 0.70 | 0.01 | 0.99 | 69.13 | 29.88 |
| 15YD-02-2-3 | 60.45 | 0.00 | 24.62 | 0.00 | 0.02 | 0.00 | 6.50 | 8.06 | 0.15 | 99.79 | 2.70 | 1.29 | 0.31 | 0.70 | 0.01 | 0.84 | 68.60 | 30.56 |
| 15YD-02-2-4 | 58.32 | 0.00 | 25.68 | 0.15 | 0.05 | 0.01 | 8.18 | 7.28 | 0.15 | 99.83 | 2.62 | 1.36 | 0.39 | 0.63 | 0.01 | 0.85 | 61.17 | 37.98 |
| 15YD-02-2-5 | 57.86 | 0.00 | 26.22 | 0.05 | 0.00 | 0.02 | 8.37 | 6.83 | 0.14 | 99.50 | 2.60 | 1.39 | 0.40 | 0.60 | 0.01 | 0.81 | 59.16 | 40.03 |
| 15YD-02-2-6 | 57.97 | 0.01 | 26.03 | 0.06 | 0.03 | 0.00 | 8.28 | 6.98 | 0.11 | 99.48 | 2.61 | 1.38 | 0.40 | 0.61 | 0.01 | 0.63 | 60.03 | 39.35 |
| 15YD-02-2-7 | 58.57 | 0.00 | 25.82 | 0.02 | 0.00 | 0.04 | 7.46 | 7.28 | 0.09 | 99.28 | 2.63 | 1.37 | 0.36 | 0.63 | 0.00 | 0.50 | 63.53 | 35.97 |
| 15YD-02-2-8 | 59.75 | 0.00 | 25.05 | 0.15 | 0.01 | 0.00 | 7.01 | 7.45 | 0.12 | 99.54 | 2.67 | 1.32 | 0.34 | 0.65 | 0.01 | 0.68 | 65.34 | 33.99 |
| 15YD-02-1-1 | 59.78 | 0.01 | 25.01 | 0.06 | 0.00 | 0.00 | 7.09 | 7.90 | 0.07 | 99.92 | 2.67 | 1.32 | 0.34 | 0.68 | 0.00 | 0.39 | 66.59 | 33.02 |
| 15YD-02-1-2 | 59.59 | 0.00 | 25.16 | 0.04 | 0.00 | 0.04 | 7.03 | 7.65 | 0.13 | 99.65 | 2.67 | 1.33 | 0.34 | 0.66 | 0.01 | 0.76 | 65.82 | 33.42 |
| 15YD-02-1-3 | 58.44 | 0.01 | 25.92 | 0.09 | 0.00 | 0.00 | 7.93 | 7.31 | 0.11 | 99.81 | 2.62 | 1.37 | 0.38 | 0.64 | 0.01 | 0.62 | 62.13 | 37.25 |
| 15YD-02-1-4 | 58.61 | 0.00 | 26.22 | 0.00 | 0.00 | 0.00 | 7.96 | 7.20 | 0.08 | 100.07 | 2.62 | 1.38 | 0.38 | 0.62 | 0.00 | 0.47 | 61.78 | 37.74 |
| 15YD-02-1-5 | 60.38 | 0.03 | 24.61 | 0.01 | 0.12 | 0.03 | 6.64 | 7.99 | 0.09 | 99.88 | 2.69 | 1.29 | 0.32 | 0.69 | 0.00 | 0.49 | 68.22 | 31.30 |
| 15YD-02-2-1 | 58.49 | 0.00 | 25.96 | 0.01 | 0.00 | 0.00 | 7.95 | 6.93 | 0.09 | 99.43 | 2.63 | 1.37 | 0.38 | 0.60 | 0.01 | 0.51 | 60.91 | 38.58 |
| 15YD-02-1-2 | 58.78 | 0.01 | 26.02 | 0.02 | 0.01 | 0.00 | 7.82 | 7.18 | 0.15 | 99.97 | 2.63 | 1.37 | 0.37 | 0.62 | 0.01 | 0.85 | 61.88 | 37.27 |
| 15YD-02-1-3 | 59.24 | 0.04 | 25.56 | 0.11 | 0.00 | 0.00 | 7.70 | 7.46 | 0.19 | 100.29 | 2.64 | 1.34 | 0.37 | 0.64 | 0.01 | 1.08 | 63.00 | 35.93 |

为 $5.94 \times 10^8 \sim 6.10 \times 10^8$ Pa, 平均压力 6.01×10^8 Pa。按 0.1 GPa 相当于 3.3 km 计算, 寄主岩角闪石平均侵位深度为 20.6 km, MMEs 中角闪石平均侵位深度为 19.8 km, 以上估算结果表明两者形成的压力条件比较接近, 反映寄主岩和 MMEs 是在近似的环境中形成。

4.2 岩石成因及岩浆源区

目前关于花岗岩岩石类型的划分, 最常见的方案是 ISMA 型分类 (Chappell and White, 1974), 而真正由地幔衍生出的 M 型花岗岩极少, 所以自然界中出现的主要是 I 型、S 型和 A 型花岗岩。从矿物学

特征上来说, 寄主岩普遍含有角闪石矿物 (图 3e), 而角闪石被认为是 I 型花岗岩的矿物学标志, 同时副矿物组合中普遍存在榍石、磁铁矿, 而未见堇青石、白云母、石榴子石等富铝矿物。寄主岩为准铝质岩石, A/CNK 值小于 1.1, CIPW 标准矿物中不出现刚玉或者刚玉含量小于 1%, 区别于 S 型花岗岩 (Chappell and White, 1974)。此外, Rb/Sr 比值能够有效地提供源区性质的信息, Rb/Sr < 0.9 为 I 型花岗岩, Rb/Sr > 0.9 为 S 型花岗岩 (王德滋等, 1993)。寄主岩的 Rb/Sr 比值介于 0.29~0.40 (小于 0.9), 同时 P_2O_5 随 SiO_2 的增加而呈现降低趋势 (表 2, 图 7), 与

表4 暗色微粒包体和寄主岩中角闪石电子探针分析结果(%)
Table 4 EMPA results(%) of hornblendes in enclaves and host rocks

| Samples | 15YD-01-2-1 | 15YD-01-2-2 | 15YD-01-3-1 | 15YD-01-3-2 | 15YD-02-2-1 | 15YD-02-2-2 |
|--------------------------------|-------------|-------------|-------------|-------------|-------------|-------------|
| | 暗色微粒包体 | | | 寄主岩 | | |
| SiO ₂ | 42.24 | 42.36 | 42.41 | 42.28 | 41.99 | 42.27 |
| TiO ₂ | 0.85 | 0.86 | 0.91 | 0.92 | 0.83 | 0.84 |
| Al ₂ O ₃ | 10.46 | 10.66 | 10.53 | 10.71 | 10.98 | 10.81 |
| FeO | 20.74 | 20.22 | 20.87 | 20.39 | 21.13 | 21.28 |
| MnO | 0.60 | 0.64 | 0.52 | 0.51 | 0.55 | 0.78 |
| MgO | 8.12 | 8.58 | 8.25 | 8.50 | 8.05 | 7.96 |
| CaO | 11.36 | 11.56 | 11.59 | 11.71 | 11.52 | 11.63 |
| Na ₂ O | 0.32 | 0.41 | 0.39 | 0.36 | 0.33 | 0.32 |
| K ₂ O | 1.32 | 1.17 | 1.41 | 1.18 | 1.06 | 1.22 |
| 以 23 个 O 计算的阳离子数 | | | | | | |
| Si | 6.45 | 6.42 | 6.43 | 6.41 | 6.37 | 6.39 |
| Al ^{IV} | 1.55 | 1.58 | 1.57 | 1.59 | 1.63 | 1.61 |
| Al ^{VII} | 0.33 | 0.32 | 0.32 | 0.32 | 0.33 | 0.32 |
| Ti | 0.10 | 0.10 | 0.10 | 0.11 | 0.10 | 0.10 |
| Fe ³⁺ | 0.96 | 0.96 | 0.89 | 0.92 | 1.06 | 1.00 |
| Fe ²⁺ | 1.69 | 1.60 | 1.76 | 1.66 | 1.62 | 1.69 |
| Mn | 0.08 | 0.08 | 0.07 | 0.07 | 0.07 | 0.10 |
| Mg | 1.85 | 1.94 | 1.87 | 1.92 | 1.82 | 1.80 |
| Ca | 1.86 | 1.88 | 1.88 | 1.90 | 1.87 | 1.88 |
| Na | 0.09 | 0.12 | 0.11 | 0.11 | 0.10 | 0.09 |
| K | 0.26 | 0.23 | 0.27 | 0.23 | 0.20 | 0.23 |
| P (kbar) | 5.94 | 6.05 | 5.95 | 6.10 | 6.34 | 6.16 |
| H (km) | 19.63 | 20.12 | 19.62 | 19.96 | 20.91 | 20.32 |

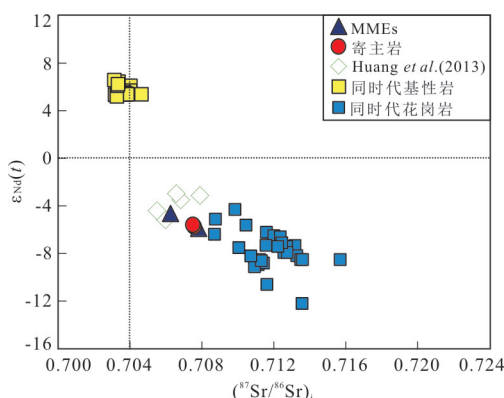


图9 寄主岩及其MMEs(⁸⁷Sr/⁸⁶Sr)_i-ε_{Nd}(t)图解
Fig.9 (⁸⁷Sr/⁸⁶Sr)_i-ε_{Nd}(t) diagram of granodiorites and enclaves in the Ba'er pluton

晚侏罗世花岗岩数据引自 Li *et al.* (2007), Xu *et al.* (2007); 晚侏罗世基性岩数据引自 Meng *et al.* (2012), Wang *et al.* (2003, 2008), Gan *et al.* (2018)

S型花岗岩演化趋势具有明显差异,与I型花岗岩演化趋势一致。另外,寄主岩也具有明显不同于A型花岗岩的一系列地球化学特征,主要表现在:(1)寄主岩中FeO_t/MgO的比值较低(为1.2~2.8),区别于A型花岗岩显著富铁的特征(FeO_t/MgO>10, Whalen *et al.*, 1987);(2)寄主岩的10⁴×Ga/Al(2.26~2.31)的值明显低于A型花岗岩的10⁴×Ga/Al的比值(>2.60, Whalen *et al.*, 1987);(3)前文已经提及寄主岩的锆石饱和温度为730~754℃(表2),平均值为740℃,相较于A型花岗岩的锆石饱和温度偏低(通常高于800℃)。综合上述矿物学和地球化学特征,八二花岗质岩体中寄主岩为准铝质I型花岗岩。

实验岩石学表明,地壳中的变基性岩石部分熔融可以形成准铝质花岗岩(Beard and Lofgren, 1991; Johannes and Holtz, 1996; Sisson *et al.*, 2004);泥沙质沉积岩类部分熔融形成强烈富铝和富钾的花岗岩(Patiño Douce and Harris, 1998);地壳碎屑沉积岩类部分熔融形成偏酸性的过铝质花岗岩(Johannes and Holtz, 1996; Patiño Douce and Harris, 1998)。同时前人的研究进一步表明,变质玄武岩在压力较高时部分熔融会产生具有高Na₂O的熔体(Rapp and Watson, 1995)。寄主I型花岗质岩石的SiO₂含量较低(61.04%~65.84%),富Na₂O(3.17%~3.66%),A/CNK=0.94~1.00,为准铝质系列花岗岩,在不同源岩部分熔融产生花岗质岩石的相关图解中,样品点基本落入斜长角闪岩部分熔融形成的熔体区域内(图10),通常下地壳变基性岩熔融产生不了富钾的花岗质岩石,除非源岩是本身富钾的变基性岩(Huang *et al.*, 2013)。寄主岩具有高钾钙碱性的特征,因此源区中可能混杂一定量钾含量高的变沉积岩。结合八二花岗质岩体较高的初始Sr同位素比值(寄主岩:0.707 63~0.707 67,MMEs:0.707 04~0.707 74)、比较低的ε_{Nd}(t)值(寄主岩:-5.73~-5.67,MMEs:-5.81~-4.35)以及二阶段模式年龄(1.12~1.40 Ga),表明源区主体应为中元古代华南中下地壳中的变基性岩部分熔融形成。寄主岩的Rb/Sr比值范围为0.29~0.40,明显大于幔源岩浆成因花岗岩(Rb/Sr<0.05),而与壳幔混合源花岗岩(Rb/Sr=0.05~0.5)范围一致(张瑞刚等, 2018)。同时原始地幔的Nb/Ta值远高于地壳,而MMEs的Nb/Ta值(平均16.2,n=5)明显高于寄主岩的Nb/Ta(平均9.4,n=5)值,并处于原始

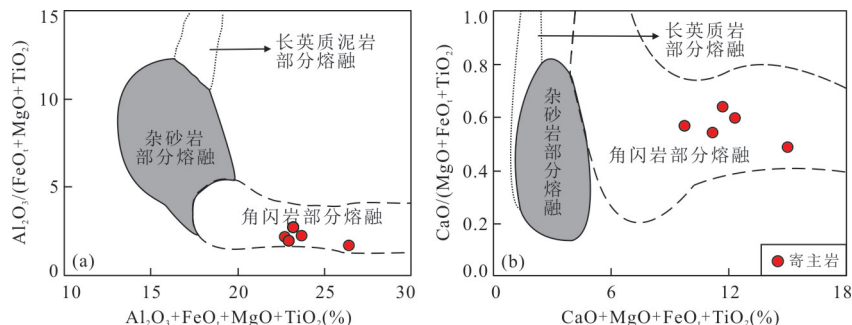


图 10 不同源岩脱水部分熔融实验获得的熔体图解

Fig. 10 Experimental results of partial melts from different source rock types

a,b 据 Wang et al. (2016)

地幔(19.9 ± 0.6 , Münker *et al.*, 2003)和下地壳值(8.3, Rudnick and Gao, 2003)之间,综上表明,八二花岗质岩体的母岩浆起源于镁铁质—中性下地壳的部分熔融,并且可能有少量幔源物质参与到成岩过程。

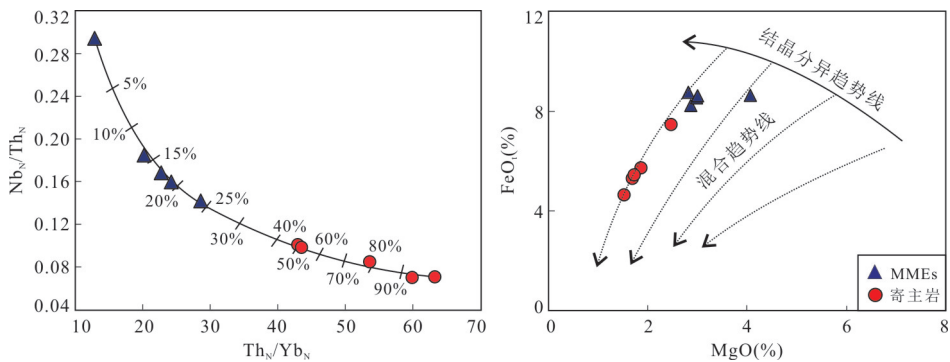
4.3 MMEs 成因

前人关于花岗岩中的MMEs的成因提出了多种模式,例如残留体、捕虏体、同源包体、壳幔岩浆混合体。本文MMEs具有典型的岩浆结构,未见变晶结构和片理构造等变质岩组构特征,同时寄主岩与MMEs均为准铝质岩石,未见富铝变质矿物(如石榴石、红柱石、夕线石和堇青石等),说明MME不是基底变质岩难熔物质的残留体。同时MMEs多呈塑性变形,未见固态下热变质现象,且锆石U-Pb年龄显示MMEs与寄主岩年龄在误差范围内一致,说明这些MMEs不是围岩捕掳体。此外,如果MMEs包体和寄主岩石是由同源岩浆分异形成,则其同种矿物的粒度应与寄主岩相近,但镜下观察到矿物的粒度却明显小于其寄主岩。其次,如果MMEs是花岗质岩浆早期结晶分异产物的堆积体,由于REE为强不相容元素,则其REE含量相比寄主岩应明显偏低,但实际MMEs与寄主岩的稀土元素总量基本一致;同时,同源岩浆的分异演化过程中,随着长石类矿物的分离结晶,晚期岩浆的铕负异常将更加明显,而本文自MMEs至寄主花岗岩,样品的铕负异常不但没有增大的趋势,反而有的样品还变小(表2),表明它不是寄主岩浆早期的堆晶体或析离体。

从野外宏观上看,八二花岗质岩体发育以球形一半球形为主的MMEs, Vernon *et al.*(1988)认为球形一半球形的MMEs是反映岩浆混合和流动的有利证据,并且可以观察到存在较大的MMEs里包

含着较小的MMEs,且内部MMEs粒度大小不一,这可能是岩浆的不均一混熔的结果(李增达等,2018)。这些现象可能说明了MMEs形成的某个阶段处于液态,具有一定的流动性,由于运动中相对速度的差异,而使处于不同演化程度的MMEs移至相近的区域内,部分大的MMEs偶尔捕获较小的包体就形成了“双包体”(图2c)。岩相学研究表明,八二MMEs的粒度较细,含斜长石斑晶,可见斜长石斑晶里包裹有大量早期快速结晶的暗色微粒矿物。同时在MMEs中常见针状磷灰石(图3f),反映MMEs是在一种淬火条件下快速冷凝结晶的,而针状磷灰石作为岩浆快速冷凝的标志被认为是发生岩浆混合作用的常见矿物标志(Hibbard, 1991)。

在Harker图解上(图7),寄主岩和MMEs的主量元素具有良好的线性关系,呈现出典型的岩浆混合或者结晶分异演化的趋势(肖庆辉等, 2002)。在微量元素方面,寄主岩和MMEs的微量元素蛛网图和稀土元素配分图型式均十分相似(图6),显示出MMEs和寄主岩的成分可能在混合的过程中趋于均一。 Th_N/Yb_N - Nb_N/Th_N 图解可以模拟两端元混合时成分变化的情况(曾认宇等, 2016),由于原始端元的成分无法获得,所以选取 Th_N/Yb_N 值最小的MMEs和 Th_N/Yb_N 值最大的寄主岩作为初始的端元进行拟合,如图11a所示,MMEs和寄主岩的样品均落在拟合线附近。在 $\text{MgO}-\text{FeO}_i$ 图解中(图11b),寄主岩和MMEs的样品沿混合趋势线分布,也反映出该岩体具有岩浆混合成因的特征。另外Sr-Nd同位素也是判断寄主岩和MMEs源区的重要依据,但即使是目前许多岩浆混合成因MMEs的研究当中,寄主岩与MMEs的Sr-Nd同位素表现出显著差异的也非常少,且常常趋于一致(高永宝等, 2015; 李

图 11 Th_N/Yb_N - Nb_N/Th_N 关系图(a)和 MgO - FeO_t 图(b)Fig.11 Diagrams of Th_N/Yb_N - Nb_N/Th_N (a) and MgO - FeO_t (b)图 a 据曾认宇等(2016);图 b 据 Zorpi *et al.*(1989)

增达等, 2018), 可能是寄主岩和 MMEs 的全岩 Sr-Nd 同位素容易受到岩浆混合作用的影响。综上所述, 八二花岗质岩体中的 MMEs 更可能为岩浆混合成因, 即由镁铁质岩浆与长英质岩浆混合形成。

4.4 构造背景讨论

华南板块是现今组成东亚诸多地块中最主要的一个块体, 具复杂的构造演化史, 目前一般认为华南板块是由其东南部的华夏陆块和西北部的扬子陆块在新元古代发生碰撞—拼合形成(Li *et al.*, 2008; Zhang *et al.*, 2012b; Yao *et al.*, 2015; 张玉芝等, 2015; Zhang and Wang, 2016; Wang *et al.*, 2018)。华南板块自显生宙以来主要经历了 3 期重要的构造—热事件(广西运动、印支运动和燕山运动; Wang *et al.*, 2005, 2007, 2011, 2013; Zhou *et al.*, 2006; Charvet *et al.*, 2010; Zhang *et al.*, 2012a; Charvet, 2013), 出露了巨量的花岗岩, 被视为一个“大花岗岩省”(王德滋和周金城, 2005)。其中中生代岩浆活动最为强烈, 以晚侏罗世岩浆岩为代表, 这些晚侏罗世岩浆岩主要分布在华南板块的内陆区域, 岩石类型以黑云母二长花岗岩以及黑云母正长花岗岩为主(孙涛, 2006; Zhou *et al.*, 2006; Wang *et al.*, 2013), 少量分布于东南沿海地区(张玉芝等, 2015)。关于华南地区晚侏罗世岩浆活动的成因机制和构造背景, 一部分学者认为华南板块中生代处于活动大陆边缘环境, 其岩浆活动与古太平洋板块俯冲作用密切相关(Sylvester, 1998; Zhou and Li, 2000; Zhou *et al.*, 2006; Li and Li, 2007; Jiang *et al.*, 2009, 2015), 而另一部分学者认为该时期的岩浆活动形成于陆内环境, 与古太平洋的俯冲无直接联系(Wang *et al.*, 2003, 2008, 2013; Chen *et al.*, 2008; 陈新跃等, 2013; Gan *et al.*, 2016)。

在桂东和粤西地区分布有一系列中晚侏罗世的钾玄质岩石, 包括桂东右江盆地的钾玄质高镁安山岩(~ 159 Ma; 甘成势等, 2016)、桂东横县马山钾玄质岩石($\sim 154\sim 166$ Ma; 劳妙姬等, 2015; Gan *et al.*, 2018)、桂东南南渡钾玄质岩石(~ 162 Ma; 陈新跃等, 2013)、粤西阳春地区中晚侏罗世钾玄质岩石($\sim 154\sim 164$ Ma; 李献华等, 2000, 2001)。同时在该地区以及湘东南地区出露有一系列晚侏罗世 A 型花岗岩和基性岩(Wang *et al.*, 2003, 2008; 付建明等, 2004; Jiang *et al.*, 2009, 2015 Huang *et al.*, 2011; Gan *et al.*, 2016)。这些钾玄质岩石、A 型花岗岩和基性岩的出露暗示该地区晚侏罗世处于伸展环境。在粤西南邻近本次研究区域的小梁岩体和岗尾岩体($159\sim 165$ Ma), 与本文花岗岩特征类似, 均为 I 型花岗岩, 被认为是软流圈地幔物质上涌导致地壳物质部分熔融后的产物, 同样形成于陆内伸展环境(Huang *et al.*, 2013)。因此, 结合区域构造演化, 阳江市八二寄主岩与 MMEs 更可能形成于远离岛弧的板内伸展环境。由于岩石圈的伸展以及软流圈的上涌底侵, 大量的热量导致以变基性岩成分为主的中下地壳发生部分熔融, 混以少量的幔源物质, 产生了中基性的母岩浆, 且在上升侵位过程中发生不同程度的分离结晶作用, 这个过程反映了该区晚侏罗世岩石圈伸展—减薄的过程。

5 结论

(1) 八二花岗质岩体中寄主岩和 MMEs 的 LA-ICP-MS 锆石 U-Pb 年龄分别为 160.0 ± 1.0 Ma (MSWD=0.1) 和 159.3 ± 1.1 Ma (MSWD=0.3), 形成于晚侏罗世。锆石饱和温度计和角闪石全铝压

力计表明八二花岗质岩体结晶于730~754 °C和19.8~20.6 km。

(2)八二花岗质岩体的主体为中粗粒不等粒花岗质岩石,属于准铝质的I型花岗岩,其中发育的MMEs是同时期产物,局部可能存在岩浆混合作用。

(3)八二花岗质岩体形成于板内伸展环境,由于软流圈物质上涌底侵,导致中下地壳变基性岩为主的源岩部分熔融,并且源区有少量幔源物质的加入。

致谢:本项目受到国家自然科学基金项目(U1701641, 41830211)、中国科学技术部国家重点研发计划课题(2016YFC0600303)和广东省自然科学基金项目(2018B030312007)资助。感谢审稿专家提出的建设性意见,对提高本文质量起到了重要作用。

References

- Barbarin, B., 2005. Mafic Magmatic Enclaves and Mafic Rocks Associated with Some Granitoids of the Central Sierra Nevada Batholith, California: Nature, Origin, and Relations with the Hosts. *Lithos*, 80(1–4): 155–177. <https://doi.org/10.1016/j.lithos.2004.05.010>
- Beard, J. S., Lofgren, G. E., 1991. Dehydration Melting and Water - Saturated Melting of Basaltic and Andesitic Greenstones and Amphibolites at 1, 3, and 6.9 kb. *Journal of Petrology*, 32(2): 465–401. <https://doi.org/10.1093/petrology/32.2.365>
- Blake, S., Fink, J.H., 2000. On the Deformation and Freezing of Enclaves during Magma Mixing. *Journal of Volcanology and Geothermal Research*, 95(1–4): 1–8. [https://doi.org/10.1016/s0377-0273\(99\)00129-8](https://doi.org/10.1016/s0377-0273(99)00129-8)
- Boehnke, P., Watson, E. B., Trail, D., et al., 2013. Zircon Saturation Re-Revisited. *Chemical Geology*, 351: 324–334. <https://doi.org/10.1016/j.chemgeo.2013.05.028>
- Chappell, B. W., 1996. Magma Mixing and the Production of Compositional Variation within Granite Suites: Evidence from the Granites of Southeastern Australia. *Journal of Petrology*, 37(3): 449–470. <https://doi.org/10.1093/petrology/37.3.449>
- Chappell, B. W., White, A. J.R., 1974. Two Contrasting Granite Type. *Pacific Geology*, (8):173–174.
- Charvet, J., 2013. The Neoproterozoic – Early Paleozoic Tectonic Evolution of the South China Block: An Overview. *Journal of Asian Earth Sciences*, 74(18): 198–209. <https://doi.org/10.1016/j.jseas.2013.02.015>
- Charvet, J., Shu, L. S., Faure, M., et al., 2010. Structural Development of the Lower Paleozoic Belt of South China: Genesis of an Intracontinental Orogen. *Journal of Asian Earth Sciences*, 39(4): 309–330. <https://doi.org/10.1016/j.jseas.2010.03.006>
- Chen, C. H., Lee, C. Y., Shinjo, R., 2008. Was There Jurassic Paleo-Pacific Subduction in South China?: Constraints from $^{40}\text{Ar}/^{39}\text{Ar}$ Dating, Elemental and Sr – Nd – Pb Isotopic Geochemistry of the Mesozoic Basalts. *Lithos*, 106 (1 – 2): 83–92. <https://doi.org/10.1016/j.lithos.2008.06.009>
- Chen, J. Y., Yang, J. H., 2015. Petrogenesis of the Fogang Highly Fractionated I – Type Granitoids: Constraints from Nb, Ta, Zr and Hf. *Acta Petrologica Sinica*, 31 (3):846–854(in Chinese with English abstract).
- Chen, S., Niu, Y. L., Sun, W. L., et al., 2015. On the Origin of Mafic Magmatic Enclaves (MMEs) in Syn-Collisional Granitoids: Evidence from the Baojishan Pluton in the North Qilian Orogen, China. *Mineralogy and Petrology*, 109(5): 577–596. <https://doi.org/10.1007/s00710-015-0383-5>
- Chen, G.N., Grapes, R., 2003. An In-Situ Melting Model of Granite Formation: Geological Evidence from Southeast China. *International Geology Review*, 45(7): 611–622. <https://doi.org/10.2747/0020-6814.45.7.611>
- Chen, X. Y., Wang, Y. J., Zhang, Y. Z., et al., 2013. Geochronology and Geochemical Characteristics of the Nandu Syenite in SE Guangxi and Its Implications. *Geotectonica et Metallogenesis*, 37(2):284–293(in Chinese with English abstract).
- Clemens, J.D., Wall, V.J., 1988. Controls on the Mineralogy of S-Type Volcanic and Plutonic Rocks. *Lithos*, 21(1): 53–66. [https://doi.org/10.1016/0024-4937\(88\)90005-9](https://doi.org/10.1016/0024-4937(88)90005-9)
- Cui, J.J., Zhang, Y.Q., Dong, S.W., et al., 2013. Late Mesozoic Orogenesis along the Coast of Southeast China and Its Geological Significance. *Geology in China*, 40(1): 86–105(in Chinese with English abstract).
- Dan, W., Wang, Q., Wang, X. C., et al., 2015. Overlapping Sr – Nd – Hf – O Isotopic Compositions in Permian Mafic Enclaves and Host Granitoids in Alxa Block, NW China: Evidence for Crust – Mantle Interaction and Implications for the Generation of Silicic Igneous Provinces. *Lithos*, 230: 133–145. <https://doi.org/10.1016/j.lithos.2015.05.016>
- Didier, J., Barbarin, B., 1991. Enclaves and Granite Petrology, Developments in Petrology. Elsevier, New York.
- Elburg, M.A., 1996. Genetic Significance of Multiple Enclave Types in a Peraluminous Ignimbrite Suite, Lachlan Fold

- Belt, Australia. *Journal of Petrology*, 37(6): 1385–1408. <https://doi.org/10.1093/petrology/37.6.1385>
- Fu, J.M., Ma, C.Q., Xie, C.F., et al., 2004. The Determination of the Formation Ages of the Xishan Volcanic-Intrusive Complex in Southern Hunan Province. *Acta Geoscientia Sinica*, 25(3): 303–308(in Chinese with English abstract).
- Gan, C.S., Wang, Y.J., Zhang, Y.Z., et al., 2016. The Earliest Jurassic A-Type Granite in the Nanling Range of South-eastern South China: Petrogenesis and Geological Implications. *International Geology Review*, 59(3): 274–292. <https://doi.org/10.1080/00206814.2016.1254574>
- Gan, C. S., Zhang, Y. Z., Barry, T. L., et al., 2018. Jurassic Metasomatised Lithospheric Mantle beneath South China and Its Implications: Geochemical and Sr-Nd Isotope Evidence from the Late Jurassic Shoshonitic Rocks. *Lithos*, 320–321: 236–249. <https://doi.org/10.1016/j.lithos.2018.09.007>
- Gan, C.S., Wang, Y.J., Zhang, Y.Z., et al., 2016. The Identification and Implications of the Late Jurassic Shoshonitic High-Mg Andesite from the Youjiang Basin. *Acta Petrologica Sinica*, 32(11): 3281–3294(in Chinese with English abstract).
- Gao, Y. B., Li, K., Qian, B., et al., 2015. The Genesis of Granodiorites and Dark Enclaves from the Kaerqueka Deposit in East Kunlun Belt: Evidence from Zircon U-Pb Dating, Geochemistry and Sr-Nd-Hf Isotopic Compositions. *Geology in China*, 42(3): 646–662(in Chinese with English abstract).
- Guangdong Geological Bureau, 1988. Regional Geology of Guangdong Province. Geological Publishing House, Beijing(in Chinese).
- Hibbard, M.J., 1991. Textural Anatomy of Twelve Magma-Mixed Granitoid Systems. Enclaves and Granite Petrology. Elsevier, Amsterdam, 31–444.
- Hu, Z. C., Liu, Y. S., Gao, S., et al., 2012. A “Wire” Signal Smoothing Device for Laser Ablation Inductively Coupled Plasma Mass Spectrometry Analysis. *Spectrochimica Acta Part B: Atomic Spectroscopy*, 78(78): 50–57. <https://doi.org/10.1016/j.sab.2012.09.007>
- Hu, R.Z., Bi, X.W., Peng, J.T., et al., 2007. Some Problems Concerning Relationship between Mesozoic - Cenozoic Lithospheric Extension and Uranium Metallogenesis in South China. *Mineral Deposits*, 26(2): 139–152(in Chinese with English abstract).
- Huang, H. Q., Li, X. H., Li, W. X., et al., 2011. Formation of High ^{18}O Fayalite-Bearing A-Type Granite by High-Temperature Melting of Granulitic Metasedimentary Rocks, Southern China: REPLY. *Geology*, 40(10): e278–e278. <https://doi.org/10.1130/g33526y.1>
- Huang, H. Q., Li, X. H., Li, Z. X., et al., 2013. Intraplate Crustal Remelting as the Genesis of Jurassic High-K Granites in the Coastal Region of the Guangdong Province, SE China. *Journal of Asian Earth Sciences*, 74: 280–302. <https://doi.org/10.1016/j.jseas.2012.09.009>
- Jia, X. H., Xie, G. G., Meng, D. L., et al., 2018. Petrogenesis and Implications of the Haiyan A-Type Granites and Mafic Microgranule Enclaves in Southern Guangdong Province. *Earth Science*, 43(7): 2294–2309(in Chinese with English abstract).
- Jiang, Y. H., Jiang, S. Y., Dai, B. Z., et al., 2009. Middle to Late Jurassic Felsic and Mafic Magmatism in Southern Hunan Province, Southeast China: Implications for a Continental Arc to Rifting. *Lithos*, 107(3–4): 185–204. <https://doi.org/10.1016/j.lithos.2008.10.006>
- Jiang, Y.H., Wang, G.C., Liu, Z., et al., 2015. Repeated Slab Advance – Retreat of the Palaeo-Pacific Plate underneath SE China. *International Geology Review*, 57(4): 472–491. <https://doi.org/10.1080/00206814.2015.1017775>
- Jochum, K. P., McDonough, W. F., Palme, H., et al., 1989. Compositional Constraints on the Continental Lithospheric Mantle from Trace Elements in Spinel Peridotite Xenoliths. *Nature*, 340(6234): 548–550. <https://doi.org/10.1038/340548a0>
- Johannes, W., Holtz, F., 1996. Petrogenesis and Experimental Petrology of Granitic Rocks. Springer, Berlin Heidelberg, 149–150.
- Lalonde, A. E., Bernard, P., 1993. Composition and Color of Biotite from Granites: Two Useful Properties in the Characterization of Plutonic Suites from the Hepburn Internal Zone of Wopmay Orogen, Northwest Territories. *Stroke A Journal Of Cerebral Circulation*, 46(7): 1787.
- Lao, M.J., Zou, H.P., Du, X.D., et al., 2015. Geochronology and Geochemistry of the Mashan Late Jurassic Shoshonitic Intrusives in Hengxian, Guangxi: With a Discussion on Yanshanian Tectonic Settings of the Southwestern Segment of Qinzhou-Hangzhou Metallogenic Belt. *Earth Science Frontiers*, 22(2): 95–107(in Chinese with English abstract).
- Leake, B. E., 1997. Nomenclature of Amphiboles. *Mineralogical Magazine*, 42(324): 1023–1052.
- Lee, C. T. A., Morton, D. M., 2015. High Silica Granites: Terminal Porosity and Crystal Settling in Shallow Magmatic Chambers. *Earth and Planetary Science Letters*, 409: 23–31. <https://doi.org/10.1016/j.epsl.2015.01.031>

- epsl.2014.10.040
- Li, X.H., Hu, R.Z., Rao, B., 1997. Chronology and Geochemistry of Cretaceous Mafic Dikes from Northern Guangdong, SE China. *Geochimica*, 26(2), 14—31(in Chinese with English abstract).
- Li, X.H., Li, W.X., Li, Z.X., et al., 2007. Re - Discussion on the Genetic Type and Tectonic Significance of Early Granite in Yanshan, Nanling. *Chinese Science Bulletin*, 52(9):981—991(in Chinese with English abstract).
- Li, X. H., Li, W. X., Li, Z. X., et al., 2008. 850—790 Ma Bimodal Volcanic and Intrusive Rocks in Northern Zhejiang, South China: A Major Episode of Continental Rift Magmatism during the Breakup of Rodinia. *Lithos*, 102(1—2): 341—357. <https://doi.org/10.1016/j.lithos.2007.04.007>
- Li, X. H., Li, Z. X., Li, W. X., et al., 2007. U - Pb Zircon, Geochemical and Sr - Nd - Hf Isotopic Constraints on Age and Origin of Jurassic I- and A-Type Granites from Central Guangdong, SE China: A Major Igneous Event in Response to Foundering of a Subducted Flat-Slab?. *Lithos*, 96(1—2): 186—204. <https://doi.org/10.1016/j.lithos.2006.09.018>
- Li, Z.X., Li, X.H., 2007. Formation of the 1300-km-Wide Intracontinental Orogen and Postorogenic Magmatic Province in Mesozoic South China: A Flat-Slab Subduction Model. *Geology*, 35(2): 179. <https://doi.org/10.1130/g23193a.1>
- Li, X.H., Qi, C.S., Liu, Y., et al., 2005. Genesis of Neo-proterozoic Bimodal Volcanic Rocks on the Western Margin of the Yangtze Block: Constraints on Hf Isotopes and Fe/Mn. *Chinese Science Bulletin*, 50(19): 2155—2160(in Chinese).
- Li, X.H., Zhou, H.W., Liu, Y., et al., 2000. Mesozoic Shoshonitic Intrusives in the Yangchun Basin, Western Guangdong, and their Tectonic Significance: I . Petrology and Isotope Geochronology. *Geochimica*, 29(6): 513—520(in Chinese with English abstract).
- Li, X.H., Zhou, H.W., Liu, Y., et al., 2001. Mesozoic Shoshonitic Intrusives in the Yangchun Basin, Western Guangdong, and Their Tectonic Significance: II . Trace Elements and Sr-Nd Isotopes. *Geochimica*, 30(1): 57—65(in Chinese with English abstract).
- Li, Z.D., Yu, X.F., Wang, Q.M., et al., 2018. Petrogenesis of Sanfoshan granite, Jiaodong: Diagenetic Physical and Chemical Conditions, Zircon U-Pb Geochronology and Sr-Nd Isotope Constraints. *Acta Petrologica Sinica*, 34(2):447—468(in Chinese with English abstract).
- Liang, X.R., Wei, G.J., Li, X.H., et al., 2003. Precise Measurement of $^{143}\text{Nd}/^{144}\text{Nd}$ and Sm/Nd Ratios Using Multiple - Collectors Inductively Coupled Plasma - Mass Spectrometer (MC-ICPMS). *Geochimica*, 32(1):91—96 (in Chinese with English abstract).
- Liu, Y., Gao, S., Hu, Z., et al., 2009. Continental and Oceanic Crust Recycling - Induced Melt - Peridotite Interactions in the Trans-North China Orogen: U-Pb Dating, Hf Isotopes and Trace Elements in Zircons from Mantle Xenoliths. *Journal of Petrology*, 51(1—2): 537—571. <https://doi.org/10.1093/petrology/egp082>
- Liu, Y., Liu, H.C., 1996. Accurate Determination of More than 40 Trace Elements in Rock Samples by ICP-MS. *Geochimica*, (6):552—558(in Chinese with English abstract).
- Maniar, P. D., Piccoli, P. M., 1989. Tectonic Discrimination of Granitoids. *Geological Society of America Bulletin*, 101(5): 635—643. [https://doi.org/10.1130/0016-7606\(1989\)101<0635:tdog>2.3.co;2](https://doi.org/10.1130/0016-7606(1989)101<0635:tdog>2.3.co;2)
- Mao, J.W., Xie, G.Q., Li, X.F., et al., 2004. Mesozoic Large Scale Mineralization and Multiple Lithospheric Extension in South China. *Earth Science Frontiers*, 11(1):45—55(in Chinese with English abstract).
- Meng, L. F., Li, Z. X., Chen, H. L., et al., 2012. Geochronological and Geochemical Results from Mesozoic Basalts in Southern South China Block Support the Flat-Slab Subduction Model. *Lithos*, 132—133: 127—140. <https://doi.org/10.1016/j.lithos.2011.11.022>
- Mo, X. X., 2011. Magma and Magmatic/Igneous Rocks: A Lithoprobe into the Deep Earth and Records of the Earth's Evolution. *Chinese Journal of Nature*, 33(5): 255—259, 313(in Chinese with English abstract).
- Münker, C., Pfänder, J.A., Weyer, S., et al., 2003. Evolution of Planetary Cores and the Earth - Moon System from Nb/Ta Systematics. *Science*, 301(5629): 84—87. <https://doi.org/10.1126/science.1084662>
- Niu, Y. L., Zhao, Z. D., Zhu, D. C., et al., 2013. Continental Collision Zones are Primary Sites for Net Continental Crust Growth—A Testable Hypothesis. *Earth - Science Reviews*, 127(2): 96—110. <https://doi.org/10.1016/j.earscirev.2013.09.004>
- Niu, Z.J., Liu, Y., Di, Y.J., et al., 2014. Zoning Characteristics of the Plagioclase from the Mesozoic Trachyandesite in Wuchagou Area of the Da Hinggan Mountains and Its Geological Implications. *Acta Petrologica et Mineralogica*, 33(1):102—108(in Chinese with English abstract).
- Patino Douce, A. E., Harris, N., 1998. Experimental Constraints on Himalayan Anatexis. *Journal of Petrology*, 39(4): 689—710. <https://doi.org/10.1093/petroj/39.4.689>

- 39.4.689
- Peng, Z. L., Grapes, R., Zhuang, W. M., et al., 2011. Petrochemical Composition Characteristics of Mafic Microgranular Enclaves in Granites in SE China and Their Significance. *Earth Science Frontiers*, 18(1): 74–81(in Chinese with English abstract).
- Perugini, D., Poli, G., 2012. The Mixing of Magmas in Plutonic and Volcanic Environments: Analogies and Differences. *Lithos*, 153(8): 261–277. <https://doi.org/10.1016/j.lithos.2012.02.002>
- Pietranik, A., Koepke, J., 2014. Plagioclase Transfer from a Host Granodiorite to Mafic Microgranular Enclaves: Diverse Records of Magma Mixing. *Mineralogy and Petrology*, 108(5): 681–694. <https://doi.org/10.1007/s00710-014-0326-6>
- Qin, Z. W., Ma, C. Q., Fu, J. M., et al., 2018. The Origin of Mafic Enclaves in Xiangjia Granitic Pluton of East Kunlun Orogenic Belt: Evidence from Petrography and Geochemistry. *Earth Science*, 43(7): 2420–2437(in Chinese with English abstract).
- Rapp, R. P., Watson, E. B., 1995. Dehydration Melting of Metabasalt at 8–32 kbar: Implications for Continental Growth and Crust–Mantle Recycling. *Journal of Petrology*, 36(4): 891–931. <https://doi.org/10.1093/petrology/36.4.891>
- Rickwood, P. C., 1989. Boundary Lines within Petrologic Diagrams which Use Oxides of Major and Minor Elements. *Lithos*, 22(4): 247–263. [https://doi.org/10.1016/0024-4937\(89\)90028-5](https://doi.org/10.1016/0024-4937(89)90028-5)
- Rudnick, R. L., Gao, S., 2003. Composition of the Continental Crust. *Treatise on Geochemistry*, 33:1–64.
- Schmidt, M. W., 1992. Amphibole Composition in Tonalite as a Function of Pressure: An Experimental Calibration of the Al-in-Hornblende Barometer. *Contributions to Mineralogy and Petrology*, 110(2–3): 304–310. <https://doi.org/10.1007/bf00310745>
- Shellnutt, J. G., Jahn, B. M., Dostal, J., 2010. Elemental and Sr – Nd Isotope Geochemistry of Microgranular Enclaves from Peralkaline A-Type Granitic Plutons of the Emeishan Large Igneous Province, SW China. *Lithos*, 119(1–2): 34–46. <https://doi.org/10.1016/j.lithos.2010.07.011>
- Shu, L. S., Zhou, X. M., 2002. Late Mesozoic Tectonism of Southeast China. *Geological Review*, 48(3): 249–260(in Chinese with English abstract).
- Sisson, T. W., Ratajeski, K., Hankins, W. B., et al., 2004. Voluminous Granitic Magmas from Common Basaltic Sources. *Contributions to Mineralogy and Petrology*, 148(6): 635–661. <https://doi.org/10.1007/s00410-004-0632-9>
- Sun, S. S., McDonough, W. F., 1989. Chemical and Isotopic Systematics of Oceanic Basalts: Implications for Mantle Composition and Processes. *Geological Society, London, Special Publications*, 42(1): 313–345. <https://doi.org/10.1144/gsl.sp.1989.042.01.19>
- Sun, T., 2006. A New Map Showing the Distribution of Granites in South China and Its Explanatory Notes. *Geological Bulletin of China*, 25(3): 332–335(in Chinese with English abstract).
- Sylvester, P. J., 1998. Post-Collisional Strongly Peraluminous Granites. *Lithos*, 45(1–4): 29–44. [https://doi.org/10.1016/s0024-4937\(98\)00024-3](https://doi.org/10.1016/s0024-4937(98)00024-3)
- Vernon, R. H., Etheridge, M. A., Wall, V. J., et al., 1988. Shape and Microstructure of Microgranitoid Enclaves: Indicators of Magma Mingling and Flow. *Lithos*, 22(1): 1–11. [https://doi.org/10.1016/0024-4937\(88\)90024-2](https://doi.org/10.1016/0024-4937(88)90024-2)
- Wang, Y. J., Fan, W. M., Peng, T. P., et al., 2005. Elemental and Sr–Nd Isotopic Systematics of the Early Mesozoic Volcanic Sequence in Southern Jiangxi Province, South China: Petrogenesis and Tectonic Implications. *International Journal of Earth Sciences*, 94(1): 53–65. <https://doi.org/10.1007/s00531-004-0441-4>
- Wang, Y. J., Fan, W. M., Sun, M., et al., 2007. Geochronological, Geochemical and Geothermal Constraints on Petrogenesis of the Indosian Peraluminous Granites in the South China Block: A Case Study in the Hunan Province. *Lithos*, 96(3–4): 475–502. <https://doi.org/10.1016/j.lithos.2006.11.010>
- Wang, Y. J., Fan, W. M., Zhang, G. W., et al., 2013. Phanerozoic Tectonics of the South China Block: Key Observations and Controversies. *Gondwana Research*, 23(4): 1273–1305. <https://doi.org/10.1016/j.gr.2012.02.019>
- Wang, Y. J., He, H. Y., Cawood, P. A., et al., 2016. Geochronological, Elemental and Sr–Nd–Hf–O Isotopic Constraints on the Petrogenesis of the Triassic Post-Collisional Granitic Rocks in NW Thailand and Its Paleotethyan Implications. *Lithos*, 266–267: 264–286. <https://doi.org/10.1016/j.lithos.2016.09.012>
- Wang, Y. J., Zhang, A. M., Fan, W. M., et al., 2011. Kwangian Crustal Anatexis within the Eastern South China Block: Geochemical, Zircon U–Pb Geochronological and Hf Isotopic Fingerprints from the Gneissoid Granites of Wugong and Wuyi–Yunkai Domains. *Lithos*, 127(1–2): 239–260. <https://doi.org/10.1016/j.lithos.2011.07.027>
- Wang, D. Z., Liu, C. S., Shen, W. Z., et al., 1993. The Contrast

- between Tonglu I-Type and Xiangshan S-Type Clasto-porphyritic Lava. *Acta Petrologica Sinica*, 9(1): 44—54 (in Chinese with English abstract).
- Wang, D.Z., Xie, L., 2008. Magma Mingling: Evidence from Enclaves. *Geological Journal of China Universities*, 14 (1):16—21(in Chinese with English abstract).
- Wang, D.Z., Zhou, J.C., 2005. New Progress in the Study of Large Igneous Province. *Geological Journal of China Universities*, 11(1): 1—8(in Chinese with English abstract).
- Wang, Y.J., Fan, W.M., Cawood, P. A., et al., 2008. Sr - Nd - Pb Isotopic Constraints on Multiple Mantle Domains for Mesozoic Mafic Rocks beneath the South China Block Hinterland. *Lithos*, 106(3—4): 297—308. <https://doi.org/10.1016/j.lithos.2008.07.019>
- Wang, Y.J., Fan, W.M., Guo, F., et al., 2003. Geochemistry of Mesozoic Mafic Rocks Adjacent to the Chenzhou-Linwu Fault, South China: Implications for the Lithospheric Boundary between the Yangtze and Cathaysia Blocks. *International Geology Review*, 45(3): 263—286. <https://doi.org/10.2747/0020-6814.45.3.263>
- Wang, Y.J., Liao, C.L., Fan, W.M., et al., 2004. Early Mesozoic OIB Type Alkaline Basalt in Central Jiangxi Province and Its Tectonic Implications. *Geochimica*, 33(2): 109—117(in Chinese with English abstract).
- Wei, G.J., Liang, X.R., Li, X.H., et al., 2002. Precise Measurement of Sr Isotopic Composition of Liquid and Solid Base Using (LP)MC - ICPMS. *Geochimica*, 31 (3):295—299(in Chinese with English abstract).
- Whalen, J. B., Currie, K. L., Chappell, B. W., 1987. A - Type Granites: Geochemical Characteristics, Discrimination and Petrogenesis. *Contributions to Mineralogy and Petrology*, 95(4): 407—419. <https://doi.org/10.1007/bf00402202>
- Whitehouse, M. J., Platt, J. P., 2003. Dating High-Grade Metamorphism - Constraints from Rare-Earth Elements in Zircon and Garnet. *Contributions to Mineralogy and Petrology*, 145(1): 61—74. <https://doi.org/10.1007/s00410-002-0432-z>
- Wu, F.Y., Li, X.H., Yang, J.H., et al., 2007. Discussions on the Petrogenesis of Granites. *Acta Petrologica Sinica*, 23(6):1217—1238(in Chinese with English abstract).
- Wu, Y.B., Zheng, Y.F., 2004. Zircon Genetic Mineralogy and Its Restriction on the Interpretation of U-Pb Age. *Chinese Science Bulletin*, 49(16): 1589—1604(in Chinese).
- Xiao, Q.H., Deng, J.F., Ma, D.S., et al., 2002. The Ways of Investigation on Granitoids. Geological Publishing House, Beijing, 12—71(in Chinese).
- Xie, L., Wang, D.Z., Wang, R.C., et al., 2004. Complex Zoning Texture in Plagioclases from the Quartz Diorite Enclave in the Putuo Granitic Complex, Zhejiang Province: Record of Magma Mixing. *Acta Petrologica Sinica*, 20 (6):96—107(in Chinese with English abstract).
- Xu, X. S., Lu, W. M., He, Z. Y., 2007. Age and Generation of Fogang Granite Batholith and Wushi Diorite - Hornblende Gabbro Body. *Science in China (Series D): Earth Sciences*, 50(2): 209—220. <https://doi.org/10.1007/s11430-007-2068-3>
- Yao, W. H., Li, Z. X., Li, W. X., et al., 2015. Detrital Provenance Evolution of the Ediacaran - Silurian Nanhua Foreland Basin, South China. *Gondwana Research*, 28 (4): 1449—1465. <https://doi.org/10.1016/j.gr.2014.10.018>
- Ye, Q., Mei, L. F., Shi, H. S., et al., 2018. The Late Cretaceous Tectonic Evolution of the South China Sea Area: An Overview, and New Perspectives from 3D Seismic Reflection Data. *Earth - Science Reviews*, 187: 186—204. <https://doi.org/10.1016/j.earscirev.2018.09.013>
- Zeng, R.N., Lai, J.Q., Zhang, L.J., et al., 2016. Petrogenesis of Mafic Microgranular Enclaves: Evidence from Petrography, Whole-Rock and Mineral Chemistry of Ziyunshan Pluton, Central Hunan. *Earth Science*, 41(9):1461—1478 (in Chinese with English abstract).
- Zhang, G.W., Guo, A.L., Wang, Y.J., et al., 2013. Tectonics of South China Continent and Its Implications. *Science China: Earth Sciences*, 43(10):1553—1582(in Chinese).
- Zhang, L., Ren, Z. Y., Nichols, A. R. L., et al., 2014. Lead Isotope Analysis of Melt Inclusions by LA-MC-ICP-MS. *Journal of Analytical Atomic Spectrometry*, 29(8): 1393—1405. <https://doi.org/10.1039/c4ja00088a>
- Zhang, R.G., Gao, X., Yang, L.Q., 2013. Identification of Magma Mixing: A Case Study of the Daocheng Batholith in the Yidun Arc. *Advances in Earth Science*, 10 (10) (in Chinese).
- Zhang, Y. Z., Wang, Y. J., Fan, W. M., et al., 2012a. Geochronological and Geochemical Constraints on the Metasomatised Source for the Neoproterozoic (~825 Ma) High-Mg Volcanic Rocks from the Cangshuiyu Area (Hunan Province) along the Jiangnan Domain and their Tectonic Implications. *Precambrian Research*, 220—221: 139—157. <https://doi.org/10.1016/j.precamres.2012.07.003>
- Zhang, F.F., Wang, Y. J., Zhang, A. M., et al., 2012b. Geochronological and Geochemical Constraints on the Petro-

- genesis of Middle Paleozoic (Kwangsian) Massive Granites in the Eastern South China Block. *Lithos*, 150: 188–208. <https://doi.org/10.1016/j.lithos.2012.03.011>
- Zhang, Y. Q., Dong, S. W., Li, J. H., et al., 2012. The New Progress in the Study of Mesozoic Tectonics of South China. *Acta Geoscientica Sinica*, 33(3): 257–279(in Chinese with English abstract).
- Zhang, Y. Z., Wang, Y. J., 2016. Early Neoproterozoic (~840 Ma) Arc Magmatism: Geochronological and Geochemical Constraints on the Metabasites in the Central Jiangnan Orogen. *Precambrian Research*, 275: 1–17. <https://doi.org/10.1016/j.precamres.2015.11.006>
- Zhang, Y. Z., Wang, Y. J., Guo, X. F., et al., 2015. Geochronology and Geochemistry of Cihua Neoproterozoic High-Mg Andesites in Jiangnan Orogen and Their Tectonic Implications. *Earth Science*, 40(11): 1781–1795(in Chinese with English abstract).
- Zhao, K. D., Jiang, S. Y., Yang, S. Y., et al., 2012. Mineral Chemistry, Trace Elements and Sr – Nd – Hf Isotope Geochemistry and Petrogenesis of Cailing and Furong Granites and Mafic Enclaves from the Qitianling Batholith in the Shi-Hang Zone, South China. *Gondwana Research*, 22(1): 310–324. <https://doi.org/10.1016/j.gr.2011.09.010>
- Zhou, X. M., Li, W. X., 2000. Origin of Late Mesozoic Igneous Rocks in Southeastern China: Implications for Lithosphere Subduction and Underplating of Mafic Magmas. *Tectonophysics*, 326(3–4): 269–287. [https://doi.org/10.1016/s0040-1951\(00\)00120-7](https://doi.org/10.1016/s0040-1951(00)00120-7)
- Zhou, X. M., Sun, T., Shen, W. Z., et al., 2006. Petrogenesis of Mesozoic Granitoids and Volcanic Rocks in South China: A Response to Tectonic Evolution. *Episodes*, 29(1): 26–33. <https://doi.org/10.18814/epiugs/2006/v29i1/004>
- Zhou, X. M., 2003. My Thinking about Granite Geneses of South China. *Geological Journal of China Universities*, 9(4): 556–565(in Chinese with English abstract).
- Zhu, J. C., Wang, R. C., Zhang, P. H., et al., 2009. Zircon U – Pb Geochronological Framework of Qitianling Granite Batholith, Middle Part of Nanling Range, South China. *Science China: Earth Sciences*, 39(8): 1112–1127(in Chinese).
- Zhu, J. C., Zhang, P. H., Xie, C. F., et al., 2006a. Magma Mixing Origin of the Mafic Enclaves in Lisong Granite, NE Guangxi, Western Nanling Mountains. *Geochimica*, 35(5): 506–516(in Chinese with English abstract).
- Zhu, J. C., Zhang, P. H., Xie, C. F., et al., 2006b. Zhucon U-Pb Age Framework of Huashan-Guposhan Intrusive Belt, Western Part of Nanning Range, and Its Geological Significance. *Acta Petrologica Sinica*, 22(9): 2270–2278(in Chinese with English abstract).
- Zorpi, M. J., Coulon, C., Orsini, J. B., et al., 1989. Magma Mingling, Zoning and Emplacement in Calc-Alkaline Granitoid Plutons. *Tectonophysics*, 157(4): 315–329. [https://doi.org/10.1016/0040-1951\(89\)90147-9](https://doi.org/10.1016/0040-1951(89)90147-9)

附中文参考文献

- 陈璟元, 杨进辉, 2015. 佛冈高分异 I 型花岗岩的成因: 来自 Nb - Ta - Zr - Hf 等元素的制约. *岩石学报*, 31(3): 846–854.
- 陈新跃, 王岳军, 张玉芝, 等, 2013. 桂东南南渡正长岩年代学、地球化学特征及其构造意义. *大地构造与成矿学*, 37(2): 284–293.
- 崔建军, 张岳桥, 董树文, 等, 2013. 华南陆缘晚中生代造山及其地质意义. *中国地质*, 40(1): 86–105.
- 付建明, 马昌前, 谢才富, 等, 2004. 湘西南山花岗质火山—侵入杂岩形成时代的确定. *地球学报*, 25(3): 303–308.
- 甘成势, 王岳军, 张玉芝, 等, 2016. 右江盆地晚侏罗世钾玄质高镁安山岩的厘定及其构造意义. *岩石学报*, 32(11): 3281–3294.
- 高永宝, 李侃, 钱兵, 等, 2015. 东昆仑卡而却卡铜矿区花岗闪长岩及其暗色微粒包体成因: 镍石 U-Pb 年龄、岩石地球化学及 Sr-Nd-Hf 同位素证据. *中国地质*, 42(3): 646–662.
- 广东省地质矿产局, 1988. 广东省区域地质志. 北京: 地质出版社.
- 胡瑞忠, 毕献武, 彭建堂, 等, 2007. 华南地区中生代以来岩石圈伸展及其与铀成矿关系研究的若干问题. *矿床地质*, 26(2): 139–152.
- 贾小辉, 谢国刚, 孟德磊, 等, 2018. 粤南海宴 A 型花岗岩与镁铁质包体的成因及意义. *地球科学*, 43(7): 2294–2309.
- 劳妙姬, 邹和平, 杜晓东, 等, 2015. 广西横县马山晚侏罗世钾玄质侵入岩的年代学和地球化学研究: 兼论钦杭成矿带西南段燕山期构造背景. *地学前缘*, 22(2): 95–107.
- 李献华, 胡瑞忠, 饶冰, 1997. 粤北白垩纪基性岩脉的年代学和地球化学. *地球化学*, 26(2), 14–31.
- 李献华, 祁昌实, 刘颖, 等, 2005. 扬子块体西缘新元古代双峰式火山岩成因: Hf 同位素和 Fe/Mn 新制约. *科学通报*, 50(19): 2155–2160.
- 李献华, 李武显, 李正祥, 等, 2007. 再论南岭燕山早期花岗岩的成因类型与构造意义. *科学通报*, 52(9): 981–991.
- 李献华, 周汉文, 刘颖, 等, 2000. 粤西阳春中生代钾玄质侵入岩及其构造意义: I. 岩石学和同位素地质年代学. *地球化学*, 29(6): 513–520.
- 李献华, 周汉文, 刘颖, 等, 2001. 粤西阳春中生代钾玄质侵入岩及其构造意义: II. 微量元素和 Sr-Nd 同位素地球化

- 学. 地球化学, 30(1):57—65.
- 李增达, 于晓飞, 王全明, 等, 2018. 胶东三佛山花岗岩的成因: 成岩物理化学条件、锆石 U-Pb 年代学及 Sr-Nd 同位素约束. 岩石学报, 34(2).
- 梁细荣, 韦刚健, 李献华, 等, 2003. 利用 MC-ICPMS 精确测定 $^{143}\text{Nd}/^{144}\text{Nd}$ 和 Sm/Nd 比值. 地球化学, 32(1): 91—96.
- 刘颖, 刘海臣, 1996. 用 ICP-MS 准确测定岩石样品中的 40 余种微量元素. 地球化学, (6):552—558.
- 毛景文, 谢桂青, 李晓峰, 等, 2004. 华南地区中生代大规模成矿作用与岩石圈多阶段伸展. 地学前缘, 11(1):45—55.
- 莫宣学, 2011. 岩浆与岩浆岩: 地球深部“探针”与演化记录. 自然杂志, 33(5):255—259, 313.
- 牛之建, 刘跃, 狄永军, 等, 2014. 大兴安岭五岔沟地区中生代粗安岩中斜长石环带特征及其地质意义. 岩石矿物学杂志, 33(1):102—108.
- 彭卓伦, Grapes Rodney, 庄文明, 等, 2011. 华南花岗岩暗色微粒包体的岩石化学组成特征及其意义. 地学前缘, 18 (1):74—81.
- 秦拯纬, 马昌前, 付建明, 等, 2018. 东昆仑香加花岗质岩体中镁铁质包体成因: 岩相学及地球化学证据. 地球科学, 43 (7):2420—2437.
- 舒良树, 周新民, 2002. 中国东南部晚中生代构造作用. 地质论评, 48(3):249—260.
- 孙涛, 2006. 新编华南花岗岩分布图及其说明. 地质通报, 25 (3):332—335.
- 王德滋, 周金城, 2005. 大火成岩省研究新进展. 高校地质学报, 11(1):1—8.
- 王德滋, 刘昌实, 沈渭洲, 等, 1993. 桐庐 I型和相山 S型两类碎斑熔岩对比. 岩石学报, 9(1):44—54.
- 王德滋, 谢磊, 2008. 岩浆混合作用: 来自岩石包体的证据. 高校地质学报, 14(1):16—21.
- 王岳军, 廖超林, 范蔚茗, 等, 2004. 赣中地区早中生代 OIB 碱性玄武岩的厘定及构造意义. 地球化学, 33(2): 109—117.
- 韦刚健, 梁细荣, 李献华, 等, 2002. (LP)MC-ICPMS 方法精确测定液体和固体样品的 Sr 同位素组成. 地球化学, 31(3):295—299.
- 吴福元, 李献华, 杨进辉, 等, 2007. 花岗岩成因研究若干问题. 岩石学报, 23(6):1217—1238.
- 吴福元, 李献华, 郑永飞, 等, 2008. Lu-Hf 同位素体系及其岩石学应用. 中国科学院地质与地球物理研究所学术论文汇编, 185—220.
- 吴元保, 郑永飞, 2004. 锆石成因矿物学研究及其对 U-Pb 年龄解释的制约. 科学通报, 49(16):1589—1604.
- 肖庆辉, 邓晋福, 马大铨, 等, 2002. 花岗岩研究思维与方法. 北京: 地质出版社: 12—71.
- 谢磊, 王德滋, 王汝成, 等, 2004. 浙江普陀花岗杂岩体中的石英闪长质包体: 斜长石内部复杂环带研究与岩浆混合史记录. 岩石学报, 20(6):96—107.
- 曾认宇, 赖健清, 张利军, 等, 2016. 湘中紫云山岩体暗色微粒包体的成因: 岩相学、全岩及矿物地球化学证据. 地球科学, 41(9):1461—1478.
- 张国伟, 郭安林, 王岳军, 等, 2013. 中国华南大陆构造与问题. 中国科学: 地球科学, 43(10):1553—1582.
- 张瑞刚, 高雪, 杨立强, 2018. 岩浆混合作用的识别: 以义敦岛弧稻城岩体为例. 地球科学进展, (10).
- 张玉芝, 王岳军, 郭小飞, 等, 2015. 江南中段慈化地区新元古代高镁安山岩的厘定及其构造意义. 地球科学, 40(11): 1781—1795.
- 张岳桥, 董树文, 李建华, 等, 2012. 华南中生代大地构造研究新进展. 地球学报, 33(3):257—279.
- 周新民, 2003. 对华南花岗岩研究的若干思考. 高校地质学报, 9(4):556—565.
- 朱金初, 王汝成, 张佩华, 等, 2009. 南岭中段骑田岭花岗岩基的锆石 U-Pb 年代学格架. 地球科学, 39(8):1112—1127.
- 朱金初, 张佩华, 谢才富, 等, 2006a. 桂东北里松花岗岩中暗色包体的岩浆混合作用. 地球化学, 35(5):506—516.
- 朱金初, 张佩华, 谢才富, 等, 2006b. 南岭西段花山—姑婆山侵入岩带锆石 U-Pb 年龄格架及其地质意义. 岩石学报, 22(9):2270—2278.